

MIXED WASTE CLASSIFICATION BASED ON VISION INSPECTION

HASSAN MEHMOOD KHAN

FACULTY OF ENGINEERING
UNIVERSITY OF MALAYA
KUALA LUMPUR

2022

MIXED WASTE CLASSIFICATION BASED ON VISION INSPECTION

HASSAN MEHMOOD KHAN

**DISSERTATION SUBMITTED IN FULFULMENT OF
THE REQUIREMENT FOR THE DEGREE OF
MASTER OF ENGINEERING SCIENCE**

**FACULTY OF ENGINEERING
UNIVERSITY OF MALAYA
KUALA LUMPUR**

2022

UNIVERSITY OF MALAYA

ORIGINAL LITERARY WORK DECLARATION

Name of Candidate: **Hassan Mehmood Khan**

Registration/Matric No: **KGA17035663**

Name of Degree: **Master of Engineering Science**

Title of Dissertation: **Mixed Waste Classification Based on Vision Inspection**

Field of Study:

I do solemnly and sincerely declare that:

- (1) I am the sole author/writer of this Work;
- (2) This Work is original;
- (3) Any use of any work in which copyright exists was done by way of fair dealing and for permitted purposes and any excerpt or extract from, or reference to or reproduction of any copyright work has been disclosed expressly and sufficiently and the title of the Work and its authorship have been acknowledged in this Work;
- (4) I do not have any actual knowledge nor do I ought reasonably to know that the making of this work constitutes an infringement of any copyright work;
- (5) I hereby assign all and every right in the copyright to this Work to the University of Malaya ("UM"), who henceforth shall be owner of the copyright in this Work and that any reproduction or use in any form or by any means whatsoever is prohibited without the written consent of UM having been first had and obtained;
- (6) I am fully aware that if in the course of making this Work, I have infringed any copyright whether intentionally or otherwise, I may be subject to legal action or any other action as may be determined by UM.

Candidate's Signature

Date: 18/4/22

Subscribed and solemnly declared before,

Witness's Signature

Date: 18-04-2022

Name:

Designation:

ABSTRACT

Classification of dry waste garbage is crucial since incorrect labelling of dry waste types may contribute huge loss to waste industry. An automated garbage sorting conveyor system is developed on image analysis of dry waste garbage samples which involves image acquisition, feature extraction and classification. In this study, an Automated Sorting Conveyor (ASC) integrated with Garbage Image Analysis (GIA) System with capabilities to classify and sort multiple types of garbage autonomously i.e., Crumble (Paper/Plastic), Flat (Paper/Plastic), Tin Can, Bottle (Plastic/Glass), Cup (Paper/Plastic), Plastic Box, Paper Box. A total of 640 samples of image data was collected, out of which 320 image data was used for training of machine learning model while the remaining 320 image data was used for testing purposes. Feature selection was also carried out to find the most relevant features with respect to dry garbage of interest. First, 40 features were selected with training accuracy of 79.59%. Then, better accuracy was obtained when redundant features were removed which accounted for 20 features with 81.42%. Finally, 17 features were tested and excellent accuracy of 90.69% was obtained. However, when the features F1 and F2, were removed which left with 15 features, the accuracy was reduced to 81.83%. The best 17 resulting features were used for the next process. Four classification algorithms specifically the Cubic SVM (C.SVM), Quadratic SVM (Q.SVM), Ensemble Bagged Trees (EBT) and k-Nearest Neighbor (kNN) are employed to test the classification accuracy. The Q.SVM achieved the highest training accuracy of 90.69% with 17 features in the application. Q.SVM was used for 320 testing images with the overall testing accuracy of 89.9% and the result was promising for the implementation of an ASC which is eventually crucial to cater mass recycling activities as a replacement for manual sorting.

ABSTRAK

Klasifikasi sampah buangan sangat penting kerana pelabelan jenis sampah kering yang salah dapat menyebabkan kerugian besar kepada industri sampah. Sistem penyusun penghantar sampah automatik dikembangkan pada analisis gambar sampel sampah sisa kering yang melibatkan pemerolehan gambar, pengekstrakan ciri dan klasifikasi. Dalam kajian ini, Sistem Penyusun Penghantar Automatik (ASC) yang disatukan dengan Sistem Analisis Imej Sampah (GIA) dengan keupayaan untuk mengklasifikasikan dan menyusun pelbagai jenis sampah secara automatik i.e., “Crumble (Paper/Plastic)”, “Flat (Paper/Plastic)”, “Tin Can”, “Bottle (Plastic/Glass)”, “Cup (Paper/Plastic)”, “Plastic Box” and “Paper Box”. Sebanyak 640 sampel data gambar dikumpulkan, yang mana 320 data gambar digunakan untuk latihan model pembelajaran mesin sementara 320 data gambar selebihnya digunakan untuk tujuan pengujian. Pemilihan ciri juga dilakukan untuk mencari ciri yang paling relevan berkenaan dengan sampah kering yang diminati. Pertama, 40 ciri dipilih dengan ketepatan latihan 79.59%. Kemudian, ketepatan yang lebih baik diperolehi apabila ciri berlebihan dihapus yang merangkumi 20 ciri dengan 81.42%. Akhirnya, 17 ciri diuji dan ketepatan 90.69% yang sangat baik diperolehi. Walau bagaimanapun, apabila ciri F1 dan F2, dihapus yang tersisa dengan 15 ciri, ketepatannya berkurangan menjadi 81.83%. 17 ciri terbaik yang dihasilkan digunakan untuk proses seterusnya. Empat algoritma klasifikasi khususnya “Cubic SVM (C.SVM)”, “Quadratic SVM (Q.SVM)”, “Ensemble Bagged Tree (EBT)” dan “k-Nearest Neighbor (kNN)” digunakan untuk menguji ketepatan klasifikasi. Q.SVM mencapai ketepatan latihan tertinggi sebanyak 90.69% dengan 17 ciri dalam aplikasi. Q.SVM digunakan untuk 320 imej ujian dengan ketepatan ujian keseluruhan sebanyak 89.9% dan hasilnya menjanjikan pelaksanaan ASC yang akhirnya penting untuk memenuhi aktiviti kitar semula besar-besaran sebagai pengganti untuk pengisihan manual.

ACKNOWLEDGEMENTS

In the name of Allah, Most Gracious, Most Merciful. Praise be to Allah, for given me the opportunity, ability and strength to complete this research.

Firstly, I would like to express the deepest appreciation to both my supervisors Dr. Norrima Mokhtar and Dr. Anis Salwa Khairuddin for their patience in guiding me and advises throughout the research.

My special thanks to my family especially my wife Mrs Nazish Hassan and my daughter Ms Falak Hassan, both my parents and friends for their support and encouragement till the research is completed, without them I would not be able to compete the research.

I am very thankful to Malaysian Ministry of Higher Education (MOHE) and University of Malaya for giving an opportunity to study and enhance my knowledge especially on research perspective.

TABLE OF CONTENTS

| | |
|---|-----|
| ABSTRACT | iii |
| ABSTRAK | iv |
| ACKNOWLEDGEMENTS | v |
| TABLE OF CONTENTS | vi |
| LIST OF FIGURES | ix |
| LIST OF TABLES | xii |
| LIST OF APPENDICES | xiv |
| LIST OF SYMBOLS AND ABBREVIATIONS | xv |
| CHAPTER 1: INTRODUCTION..... | 17 |
| 1.1 Problem Statement..... | 19 |
| 1.2 Research objectives | 20 |
| 1.3 Scope of the research..... | 20 |
| 1.4 Research contributions | 20 |
| 1.5 Thesis organization..... | 20 |
| CHAPTER 2: LITERATURE REVIEW..... | 22 |
| 2.1 Univariate Sorting | 22 |
| 2.1.1 Sensor-based sorting | 22 |
| 2.1.2 Air Classification..... | 22 |
| 2.2 Multivariate sorting | 22 |
| 2.2.1 Optical sensor | 22 |
| 2.3 Sorting of Different Waste | 24 |
| 2.3.1 Paper Sorting..... | 27 |

| | | |
|---|---|----|
| 2.3.2 | Plastic Sorting | 36 |
| 2.4 | Sorting Techniques | 44 |
| 2.4.1 | Image Processing..... | 44 |
| 2.5 | Research Gap..... | 58 |
| CHAPTER 3: METHODOLOGY..... | | 59 |
| 3.1 | Introduction | 59 |
| 3.2 | Project Setup..... | 60 |
| 3.2.1 | Mechanical Components | 61 |
| 3.2.2 | Electronics/Electrical Components | 61 |
| 3.2.3 | Electropneumatic Components | 63 |
| 3.2.4 | Conveyor Specifications | 64 |
| 3.3 | Image acquisition..... | 64 |
| 3.4 | Image processing | 68 |
| 3.5 | Feature Extraction..... | 71 |
| 3.5.1 | Quantile Value..... | 74 |
| 3.5.2 | Entropy | 74 |
| 3.5.3 | Standard deviation..... | 74 |
| 3.5.4 | Ratio of grey level | 75 |
| 3.5.5 | Grey level co-occurrence matrix | 76 |
| 3.6 | Classification | 78 |
| 3.6.1 | Support Vector Machine (SVM)..... | 78 |
| 3.6.2 | K-Nearest Neighbour: | 80 |
| 3.6.3 | Ensemble | 82 |
| CHAPTER 4: RESULTS AND DISCUSSION | | 84 |
| 4.1 | Training and testing dataset..... | 84 |
| 4.2 | Features Selection..... | 85 |
| 4.2.1 | First Stage of Features Selection..... | 85 |

| | | |
|-----------------------------|--|-----|
| 4.2.2 | Second Stage of Feature Selection | 88 |
| 4.2.3 | Third Stage of Feature Selection | 89 |
| 4.2.4 | Fourth Stage of Feature Selection | 89 |
| 4.3 | Classification | 91 |
| 4.3.1 | Classifier Training | 91 |
| 4.3.1.1 | Classifier Training Results for 40 Features | 92 |
| 4.3.1.2 | Classifiers Training Results for 20 Features | 93 |
| 4.3.1.3 | Classifiers Training Result for 17 Features | 94 |
| 4.3.1.4 | Classifiers Training Result for 15 Features | 95 |
| 4.3.2 | Classifier Selection | 95 |
| 4.3.3 | Classifier Performance | 98 |
| 4.4 | Discussion | 100 |
| CHAPTER 5: CONCLUSION | | 103 |
| REFERENCES | | 105 |
| APPENDIX A | | 110 |
| APPENDIX B | | 112 |
| APPENDIX C | | 116 |
| APPENDIX D | | 117 |
| APPENDIX E | | 121 |

LIST OF FIGURES

| | |
|--|----|
| Figure 1.1: GDP per capita based on purchasing power parity (PPP) [\$US]..... | 17 |
| Figure 2.1: Sequential flow chart | 27 |
| Figure 2.2: Sorting Mechanism..... | 28 |
| Figure 2.3: Block diagram of pattern classification system..... | 29 |
| Figure 2.4: Picture of pattern classification system | 30 |
| Figure 2.5: Sample images of ten classes..... | 31 |
| Figure 2.6: Subdivision of an image into square windows | 32 |
| Figure 2.7: Tukey boxplot for the area density without outliers..... | 34 |
| Figure 2.8: Tukey boxplot for the relative periodicity without outliers..... | 34 |
| Figure 2.9: Scheme of the plastic sorting system with Raman Spectroscopy..... | 39 |
| Figure 2.10: Spectra of polystyrene in (a) Raman, (b) IR and (c) NIR..... | 39 |
| Figure 2.11: Data processing flow | 40 |
| Figure 2.12: Raman spectra of PP, ABS and PS measure in 6m | 41 |
| Figure 2.13: Accuracy dependence on pre-process method..... | 41 |
| Figure 2.14: Difference of typical Raman spectrum (a) when the calculated value is less than zero, (b) when calculated value becomes highest | 42 |
| Figure 2.15: Sorting technologies for Macro-sorting and Micro-sorting..... | 43 |
| Figure 2.16: Prototype of sorting system | 45 |
| Figure 2.17: The pre-processing steps for structure identification of a plastic bottle..... | 45 |
| Figure 2.18: The experiment stages of the recognition scenario..... | 46 |
| Figure 2.19: A few samples of some correctly and incorrectly classified plastic objects..... | 48 |
| Figure 2.20: Experiments results on the classification of the PET and non-PET plastic bottles | 49 |
| Figure 2.21: Experimental results on the classification of the HDPE and PP plastic bottles | 49 |
| Figure 2.22: Piece sorting based on a machine vision | 50 |
| Figure 2.23: Rule workpiece centroid recognition..... | 51 |

| | |
|--|----|
| Figure 2.24: Qualified white regenerated parties | 52 |
| Figure 2.25: Regenerate particles mixed with different color particles | 53 |
| Figure 2.26: Sorting result..... | 53 |
| Figure 2.27: Sorting rates of three apple cultivars and their average values | 54 |
| Figure 2.28: Some defect in bottle wall and bottom | 56 |
| Figure 2.29: Some typical finish images..... | 56 |
| Figure 3.1: Overview of training and testing of the proposed system | 59 |
| Figure 3.2: Methodology Flowchart | 60 |
| Figure 3.3: Automatic Sorting Conveyor (ASC) prototype | 61 |
| Figure 3.4: Control system block diagram of the ASC system..... | 62 |
| Figure 3.5 : Electro-Pneumatics Circuit Diagram..... | 63 |
| Figure 3.6: Block diagram: Automatic Sorting Conveyor (ASC) for garbage | 64 |
| Figure 3.7: Actual system: Automatic Sorting Conveyor (ASC) for garbage | 65 |
| Figure 3.8: Inspection area of the ASC system..... | 66 |
| Figure 3.9: ASC system operational flowchart | 66 |
| Figure 3.10: Sample images from training dataset..... | 68 |
| Figure 3.11: Image processing: Segmentation process flow chart..... | 69 |
| Figure 3.12: Comparison of edge detection techniques for sample images..... | 70 |
| Figure 3.13: Segmentation stages for bottle class sample..... | 71 |
| Figure 3.14: (a) Segmentation Filter (b) Graph of summation of white pixel for each column | 72 |
| Figure 3.15: Segmentation Filter..... | 72 |
| Figure 3.16: Greyscale of Segmented Image | 73 |
| Figure 4.1: Classifiers training results for 40 Features | 92 |
| Figure 4.2: Classifiers training results for 20 Features | 93 |
| Figure 4.3: Classifiers training results for 17 Features | 94 |
| Figure 4.4: Classifiers training results for 15 Features | 95 |

Figure 4.5: Training accuracy (%) of classifiers 97

Figure 4.6: Testing Accuracy of each class for 40, 20, 17 and 15 features 102

Universiti Malaya

LIST OF TABLES

| | |
|---|----|
| Table 2.1: List of equipment | 30 |
| Table 2.2: Borders of paper color regions..... | 32 |
| Table 2.3: Specification of first stage classifiers..... | 33 |
| Table 2.4: Success rate of the modified system in %..... | 35 |
| Table 2.5: Success rates of the system with all classes in % | 35 |
| Table 2.6: Classification rate (%) of plastic types | 47 |
| Table 2.7: Confusion matrix for all classes..... | 47 |
| Table 2.8: Inspection results of defective bottle walls and bottoms | 56 |
| Table 2.9: Inspection results of good bottle walls and bottoms..... | 56 |
| Table 2.10: Inspection results of defective finish | 57 |
| Table 2.11: Inspection results of good finish..... | 57 |
| Table 2.12: Research Gap Analysis | 58 |
| Table 3.4: Number of training and testing samples for each class..... | 67 |
| Table 3.5: List of Features..... | 72 |
| Table 3.6: Grey values level for color..... | 75 |
| Table 3.7: SVM classifiers attributes | 79 |
| Table 3.8: SVM classifier types and their parameters selected..... | 79 |
| Table 3.9: KNN classifier attributes..... | 80 |
| Table 3.10: KNN parameters selected..... | 82 |
| Table 3.11: Ensemble classifier types and their attributes | 83 |
| Table 3.12: Ensemble boosted trees classifier parameters selected..... | 83 |
| Table 4.1: No of samples for each class in dataset..... | 84 |
| Table 4.2: List of 40 features for classification..... | 85 |
| Table 4.3: List of 20 features for classification..... | 89 |

| | |
|---|----|
| Table 4.4: Summary of features chosen for each stage for classifier training | 90 |
| Table 4.5: Training accuracy for each classifier for 40, 20, 17 and 15 features | 96 |
| Table 4.6: Q. SVM Classifier Testing Accuracy | 98 |
| Table 4.7: Confusion matrix of Q.SVM model testing run 3..... | 99 |
| Table 4.8: Q. SVM result summary for 40, 20, 17 and 15 features for all classes | 99 |

Universiti Malaya

LIST OF APPENDICES

| | |
|------------------|-----|
| APPENDIX A | 108 |
| APPENDIX B..... | 110 |
| APPENDIX C..... | 114 |
| APPENDIX D..... | 115 |
| APPENDIX E..... | 119 |

Universiti Malaya

LIST OF SYMBOLS AND ABBREVIATIONS

| | | |
|-------|---|--------------------------------------|
| ASC | : | Automated sorting conveyor |
| GIA | : | Garbage Image Analysis |
| SVM | : | Support vector machine |
| EBT | : | Ensemble bagged trees |
| MSW | : | Municipal solid waste |
| GDP | : | Gross domestic product |
| kNN | : | k-nearest neighbor |
| RPM | : | Revolution per minute |
| PWM | : | Pulse width modulation |
| ICSP | : | In-circuit serial programmer |
| GLCM | : | Grey level co-occurrence matrix |
| MIS | : | Magnetic induction spectroscopy |
| MOHE | : | Ministry of Higher Education |
| ELV | : | End of life – vehicle |
| CNN | : | Convolution neural networks |
| NTSC | : | National television system committee |
| NIR | : | Near infrared |
| CCD | : | Charged coupled device |
| QDA | : | Quadratic discriminant analysis |
| PCA | : | Principal component analysis |
| LDA | : | Linear discriminant analysis |
| SVD | : | Singular value decomposition |
| LEMAP | : | Laplacian Eigenmaps |
| SNR | : | Signal to noise ratio |
| IR | : | Infrared |
| PP | : | Polypropylene |
| ABS | : | Acrylonitrile Butadiene Styrene |
| PS | : | Polystyrene |

| | | |
|------|---|-------------------------------|
| PET | : | Polyethylene terephthalate |
| HDPE | : | High density polyethylene |
| IoT | : | Internet of Things |
| DNN | : | Deep Neural Network |
| PLC | : | Programmable Logic Controller |

Universiti Malaya

CHAPTER 1: INTRODUCTION

As the world moving fast towards urbanization, the most important byproduct of urban lifestyle i.e., municipal solid waste (MSW), is increasing much faster than that. There are 3 billion urban residents who generates 1.2 kg per person per day of MSW and by 2025 this amount will likely to be increased to 4.3 billion urban residents generating about 2.2 billion tons per day. The global effect of solid waste is rapidly increasing. Solid waste is a major source of methane, a potent greenhouse gas with a short-term effect. It creates air pollution and impacts on public health which cause serious diseases such as respiratory ailments, diarrhea and dengue fever (Hoorweg & Bhada-Tata, 2012).

A large quantity of solid waste production is correlated with the GDP. High GDP tends to produce large quantity of solid waste (Figure 1.1) (S. P. Gundupalli et al., 2017). Updated report data are shown by the world bank report that there are about 4 billion tons of waste generated every year globally which urban area is one of the main contributors to the huge numbers and the waste is estimated to be up until 70% by 2025. In the next 25 years, number of wastes accumulated will be rapidly increased in underdeveloped nations due to accelerated pace of urbanization and industrialization (Adedeji & Wang, 2019).

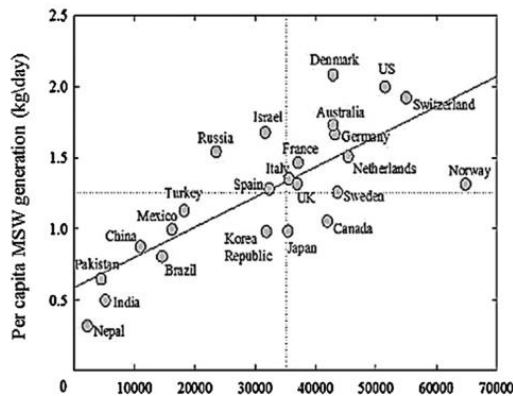


Figure 1.1: GDP per capita based on purchasing power parity (PPP) [\$US]

Solid waste is inextricably related to industrial growth and urbanization. Countries' economic prosperity rises as they urbanize. Consumption of goods and services rises in tandem with the levels of life and disposable incomes, resulting in an increase in waste generation. According to (Hoornweg & Bhada-Tata, 2012) , nearly 1.3 billion tons of MSW are produced globally per year, or 1.2 kilograms each capita per day. The real per capita figures, on the other hand, are extremely volatile, as waste generation rates vary greatly across nations, cities, and also within cities. Solid waste is traditionally thought of as a 'urban' epidemic. Rural people, on average, are wealthier, consume less store-bought goods, and reuse and recycle more. As a result, waste production rates in rural areas are much smaller. More than half of the world's population now lives in cities, and the pace of urbanization is rapidly growing. By 2050 (Hoornweg & Bhada-Tata, 2012), as many people will live in cities as the population of the whole world in 2000. This will add challenges to waste disposal. People and companies would almost definitely have to take on greater responsibility for waste generation and disposal, especially in terms of product design and waste separation. A stronger focus on 'urban extraction' is also expected to arise, as cities are the largest supplier of resources like metal and paper.

Tons of waste are created every day, creating a major problem for various cities and municipal authorities due to a lack of landfill capacity to dispose of such waste. Toxic hazard materials in the waste cause health concerns as well as environmental harm. Due to a lack of landfill space and environmental pollution, as well as its economic effects, recycling has become a major problem (Tachwali et al., 2007).

MSW is often a rich source of various useful recyclable materials such as metal, paper, plastic, and glass. Successful MSW management will result in the recovery of useful recyclable resources as well as a reduction in negative environmental effects. Waste sorting is an essential step in MSW management for materials recycling. Researcher all around the world have been looking

into automated sorting techniques for efficiently processing rising amount of MSW (S. P. Gundupalli et al., 2017).

Many research papers have been published and studies have been conducted for the MSW classification and sorting using different methods. The focus of this study is to produce prominent features and perform inspection through image analysis methods and provide effective classification models for the classification of mix commercial and residential dry wastes such as bottles, cups, plastic, paper, paper box, plastic box and tin cans. This contributes to the motivation of this work which are to improve the lacking of prominent, outstanding and discriminative features for excellent classification accuracy. However, the limitations of the study are the computing power to run the algorithm to increase more speed for the processing of the classification models and more studies can be done on the electro-pneumatic design of the sorting conveyor.

1.1 Problem Statement

According to previous studies, municipal agencies aim to have a stable and safe environment. One essential part of the target environment is waste sorting. Previous experiments, on the other hand, focused on a certain form of waste at a given point in time. From time to time, there is a new approach to tackle the problem of waste sorting for various waste materials. Finding suitable features and classification models to detect various orientation of the sample images need more attention and effort. Therefore, experiments should be carried out to find more suitable features and examine more classifiers which provide optimum and higher accuracy as compares to existing research.

1.2 Research objectives

The objectives of this research are:

- a. To develop feature extraction technique which extract prominent features from the multiple classes of MSW dry garbage images.
- b. To increase the mix garbage images classification performance.
- c. To perform inspection of garbage images for sorting applications.

1.3 Scope of the research

- i. This research focus on extracting the features from waste samples for classification purpose.
- ii. The efficiency of automatics sorting conveyor system is determined by the classification accuracy using Cubic SVM, Quadratic SVM, E. Bagged Trees and Fine. KNN models.

1.4 Research contributions

Previous works only focus to specific type of waste rather to classify and sort multiple classes of dry waste which is the discussed in this work. Furthermore, the scope of this work is to do recycling process using automatic sorting conveyor with vision-based recognition system. To overcome the current shortcoming, this work proposed multiple features which were identified and tested with multiple classifier models to classify dry solid waste garbage from public places like offices, houses and shops.

1.5 Thesis organization

This dissertation is divided into 5 chapters. The arrangement of this dissertation is:

- Chapter 1 – Introduction

This chapter explains the background of the study, problem statements, research objectives, scope of the research and research contribution.

- Chapter 2 – Literature review

Elaboration of preceding work on automatic sorting of dry garbage based on type of dry garbage waste and techniques included in this section. This chapter also discusses feature extraction and classifiers used by previous studies that motivates and encourage this research.

- Chapter 3 – Methodology

This chapter explains the proposed methodology of the research and processes involved in improving the automatic sorting conveyor for the dry garbage using vision system.

- Chapter 4 – Results and Discussion

This chapter present the results and discussion of the experiments.

- Chapter 5 – Conclusion

This chapter concludes with the analysis of the accuracy of feature extraction, classifiers and recommendation for future studies.

CHAPTER 2: LITERATURE REVIEW

Human activities produce majorly solid waste, which is a highly complex mixture. This waste can be recycled to save the environment. In recycling, sorting is the determining step. Sorting can be based on waste nature (polymer) or visual features like color, shape, or texture (Huang et al., 2010). The waste material must be categorized and organized in line with the major procedures that are used to process the material flow in order to have a cluster of parameters capable of characterizing the characteristics of material flow (Beyer & Pretz, 2004).

2.1 Univariate Sorting

2.1.1 Sensor-based sorting

Sensor-based facilities like Infrared radiation sensors can recognize only one kind of object features, i.e., waste chemical nature (Huang et al., 2010).

2.1.2 Air Classification

Product requirements, technological, and economic reasons all influence the type of classifier chosen. By producing a well-defined and stable air flow, decreasing turbulence, eliminating particle collisions, managing feed, and cleaning both fractions repeatedly, rational design and improved separation quality may be achieved. Fluidized-bed based classifiers provide steady operation and sharp separation in the cut size range of 50–1000 μ m among gravity type classifiers. Rotor classifiers can separate smaller particles, allowing for easy cut-size control and product recovery rates of up to 80% (Shapiro & Galperin, 2005).

2.2 Multivariate sorting

2.2.1 Optical sensor

Area scan cameras can capture parameters like three-dimensional shape, particle size, actual position, and color of single particles. These features can be processed using computers, and information is transferred to mechanical sorting systems. In a study, an optical sensor-based method

of solid waste processing was investigated. It was demonstrated to be a reliable multi-feature recognition tool for sorting solid waste. Almost all of the waste ingredients with actual color and shape features were recognized and then isolated due to the experiment results. Visual characteristics of single waste particles can be collected and processed quickly by 3D area scan cameras and virtual instrument software. Following the pretreatment and direct sorting methods, the sorting performance of traditional waste materials can be significantly improved by implementing optical sensor-based sorting technology (Huang et al., 2010).

A national research program centered on household samples is needed to understand the relationships between household waste arisings and socioeconomic, structural, spatial, and temporal variables (Parfitt & Flowerdew, 1997).

Sometimes sorting of waste is performed to determine waste composition. Surveys have also been performed to determine the municipal solid waste (MSW) composition resulted from household waste and civic amenity site waste. Survey findings show strong agreement on the composition of household waste but less agreement on civic amenity site waste composition. There is insufficient data to compare the commercial waste portion of municipal waste or the other components. Further study is needed to provide more accurate estimates of the composition of these streams. The use of questionnaire surveys and review of the findings indicate that a household's size and age profile influence the generation of household-collected waste. (Burnley, 2007) performed the sorting of bulk MSW samples using a rotating drum screen.

Rapid developments in industrialization and information technology have accelerated the development of the next wave of manufacturing technology. The German government identified the Industry 4.0 project in 2013 as one of ten "Future Projects" as part of its High-Tech Strategy 2020 Action Plan. Made-in-China 2025 is a plan to modernize China's economy, especially the manufacturing sector. Many applications in Industry 4.0 and Made-in-China 2025 include a combination of newly emerging new technologies, giving rise to Industry 4.0 (Xu et al., 2018).

Smart city technology incorporates the city's essential services in order to improve citizens' quality of life. In a densely populated area, segregating and disposing of garbage is a significant challenge.

Traditionally, waste was gathered manually from homes and deposited in a dump yard. The waste is disposed of by either burning it or dumping it in a landfill. As a result, more greenhouse gases are emitted, negatively impacting the atmosphere. An IoT-enabled waste segregator describes sorting municipal waste into biodegradable and non-biodegradable categories. The smart waste segregator is fitted with an infrared sensor, a moisture sensor, and a metal sensor for segregating metal, wet waste, and dry waste. The three DC motors attached to the conveyor belt are used to ensure the smooth passage of waste through the system's surface. The device has been successfully applied, and the dumped waste has been separated. The device is linked to the cloud, allowing the sensed data to be processed there for later processing. Researchers have been investigating automated sorting methods in order to increase the overall efficiency of the recycling process. One of the applications that are finding increasing demand is the Automated Sorting Conveyor (ASC), which can learn, classify and sort multiple types of garbage in an autonomous fashion (S. P. Gundupalli et al., 2017; Raj et al., 2020).

Internet-of-Things were used to create an automated waste separation system. (Pamintuan et al., 2019) created a trash can fitted with sensors that can intelligently segregate waste and provide a waste collection tracking report. Using a machine learning approach, image recognition was used to process automated trash classification. The produced prototypes were able to identify trash efficiently after training more than 2000 samples for biodegradable and non-biodegradable waste.

2.3 Sorting of Different Waste

A new method for automatic sorting of lightweight metal scrap was developed to aid in the recycling of scrap metal. The sorting separates relatively large metal pieces based on differences in apparent density and three-dimensional (3D) shape. A 3D imaging camera device comprised of a

linear laser and camera with associated optics measures shape parameters such as distance, height, length, and projected area of irregular-shaped metal pieces traveling along a conveyor. The weight and shape parameters' calculated values are passed to our own data-processing programme, which employs multivariate analysis. According to the findings, the established automatic sorting system is a highly viable method that could replace traditional dense medium separation and manual sorting.

According to the apparent density and 3D shape parameters, sorting technique could separate several hundred pieces of wrought aluminium, cast aluminium, and magnesium fragments collected from an ELV shredder facility with approximately 90% precision (Koyanaka & Kobayashi, 2010).

(Sathish Paulraj Gundupalli et al., 2017) described a method focused on thermal imaging for classifying valuable recyclables from simulated municipal solid waste (MSW) samples. The experimental results demonstrated the feasibility of combining a thermal imaging technique for classification and a robotic system for recyclable sorting in a single process stage. The recorded classification method had an 85–96% accuracy and is comparable to current single-material recyclable classification techniques. They claimed, thermal imaging-based system described in their study will emerge as a viable and low-cost large-scale classification-cum-sorting technology in recycling plants for processing MSW in developing countries.

(Kutilla et al., 2005) work described scrap metal sorting device based on color vision optical sensing and an inductive sensor array. The system's operation was tested in an actual metal recycling facility. Long-term test results showed that when the feeding conveyor speed is limited to less than 1.5 m/s, 80 percent purity can be achieved.

(O'Toole et al., 2018) paper presented a new classification method based on magnetic induction spectroscopy (MIS) for sorting three high-value metals that constitute the majority of the nonferrous fraction: copper, aluminium, and brass. Two methods are investigated: the first employs MIS with a collection of geometric features returned by a vision system. Metal fragments are matched to known test pieces from a training set; the second employs MIS only. The average

precision and recall (purity and recovery rate) were about 92 percent.

(Sakr et al., 2016) identified the form of waste-based solely on photographs. Deep learning with convolution neural networks (CNN) and support vector machines (SVM) were two common learning algorithms used (SVM). They used only a 256 x 256 coloured png image of the waste, each algorithm generates a different classifier that divides waste into three key categories: plastic, paper, and metal. The two classifiers' accuracy is compared to choose the best one and enforce it on a Raspberry Pi 3. The pi is in charge of a mechanical device that directs waste from its initial location into related container. SVM achieved a high classification accuracy of 94.8 percent, while CNN only achieved 83 percent.

(Sereda & Kostarev, 2019) performed experiment and developed relay-contact scheme to sort waste to extract fraction of recyclable waste, such as metal, plastic, glass an organic matter. They provided theoretical foundations for garbage sorting conveyor management, taking into account problems such as uneven loading and uneven waste sorting.

Deep neural networks (DNN) were employed in the classification of metals (Dang et al., 2019). They classified the region of interest (ROI) from blob detection. The goal of the blob detection was to detect a group of connected pixels inside an image (Acevedo-Avila et al., 2016; Kiran et al., 2011; Shapiro, 1996). In their study they used four deep neural network modules called the AlexNet, the GoogleNet, the VGGNet, and the ResNet. Their results showed that the proposed framework was able to classify the metal debris and the AlexNet model was most appropriate among the four models.

(Cimpan et al., 2015) reviewed physical waste processing in order to separate recyclables from MSW. The focus of the review was mostly on case studies of operational experience, with several components of automation, such as material handling, sensors, and control, being overlooked.

2.3.1 Paper Sorting

(Rahman et al., 2011) published an article that investigated the use of image processing techniques in the sorting of recyclable waste paper. In recycling, waste papers are separated into different grades before being recycled in various ways. A statistical approach with intra-class and inter-class variance techniques is used in the feature selection process to build a template database. Finally, the K-nearest neighbour (KNN) algorithm is used to identify the grade of a paper piece. The method's remarkable achievement is the precise identification and complex sorting of all grades of papers using simple image processing techniques. DNA computing methods for paper sorting have also been explored and reported by other researchers (Rahman et al., 2012).

(Md Mahmudul Hasan Russel et al., 2013) developed automatic sorter machine, which can sort various categories of waste, i.e., glass, plastic, paper, and metal. They used an electromechanical system with a microcontroller and operational amplifier. They used conventional sensors and glass sensors to sort out metal and glass waste, respectively. LDR and LASER sensors were used to sort plastic and paper waste material. The logic flow chart of the system is shown in Figure 2.1

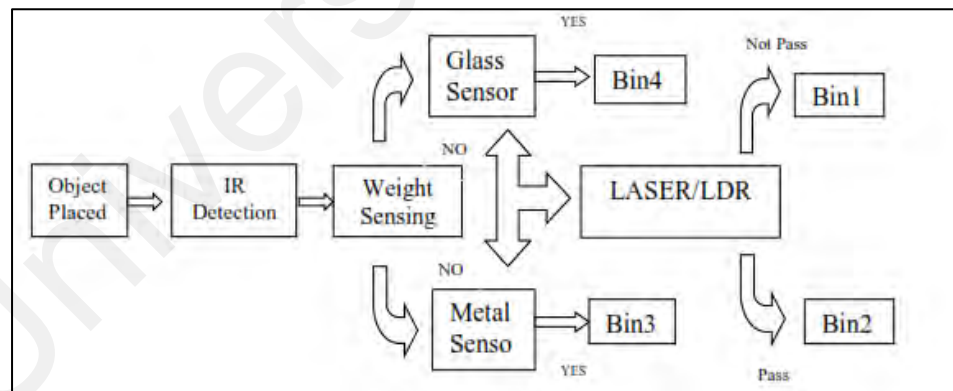


Figure 2.1: Sequential flow chart (Md Mahmudul Hasan Russel et al., 2013)

It consisted of four Bins, Bin 1 for paper, Bin 2 for Metallic elements, Bin 4 for Plastic elements, and Bin 4 for Glass particles. The object was placed in the Detection zone, and the sensor applied its sensing activity. It provided a signal to the microcontroller, and it provides the final

control signal that runs the servo motor. Servo motor run in a specific direction depending on the sensed material. The sorting mechanism is shown in Figure 2.2 (Md Mahmudul Hasan Russel et al., 2013).

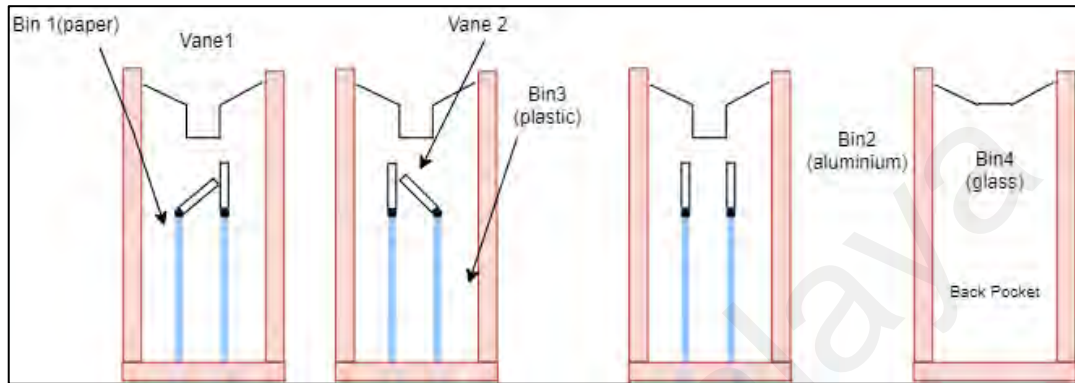


Figure 2.2: Sorting Mechanism
(Md Mahmudul Hasan Russel et al., 2013)

In this comparative study, they presented the proposed mechanism; have made the sorting procedure easy and effective, is cheaper than other trash cans available internationally, can sort out a minimum of four types of trash materials, used LDR and LASER, which replaced the conventional sensors and can use 220V as compared to other trash bins.

For future development, they mentioned system capability could be enhanced by sorting other types of material color and transparent plastic, thin and thick papers, semiconductors and conductors, rubber materials, and organics material. If manufactured at a large scale, the production cost will be low compared to manual trash bins. The response time of the system can be enhanced using an industrial-grade servo motor. It can be used to sort waste, which can be tested automatically to test the user's food habit and improve its diet.

(Gottschling & Schabel, 2016) the system uses a color video camera and dynamic scales as sensors for pattern classification. They distinguish between 10 classes of paper for recycling by extracting 26 features like weight, shape, color, texture, and number of optical brighteners. Five

classifiers of different types are trained and tested with the industrial samples, and the classification success rates lie between 94% and 100%. The picture and block diagram of their “pattern classification system” is shown in the Figures below:

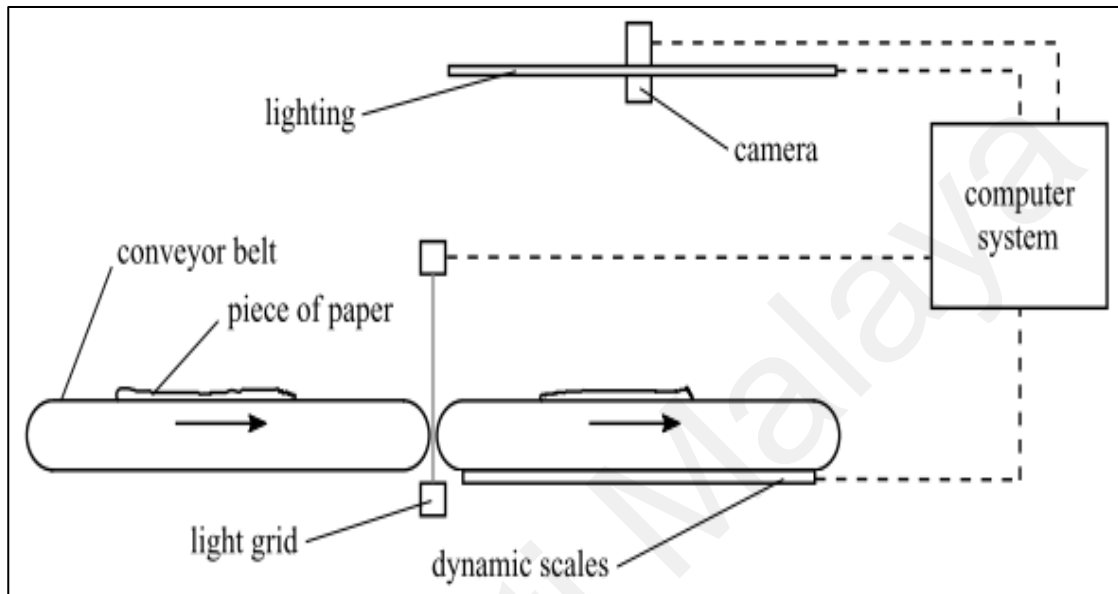


**Figure 2.3: Block diagram of pattern classification system
(Gottschling & Schabel, 2016)**

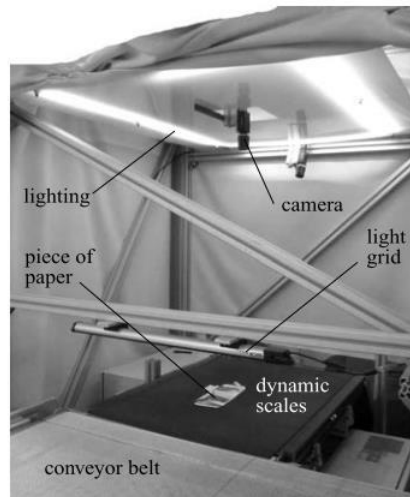


Figure 2.4: Picture of pattern classification system (Gottschling & Schabel, 2016)

The list of the equipment used is shown in Table below:

Table 2.1: List of equipment (Gottschling & Schabel, 2016)

| <i>Equipment</i> | <i>Type</i> | <i>Properties</i> |
|------------------|---|---|
| Light grid | <i>MLG-2 Prime by SICK AG</i> | Distance of the beams: 50 mm |
| Dynamic scales | <i>EC-M-SL-SI by OCS Checkweighers GmbH</i> | Precision: ± 0.5 g in the range from 0.5 to 5,000 g |
| Camera | <i>Manta G-609 by Allied Vision Technologies GmbH</i> | Resolution: $2,752 \times 2,206$ pixel |
| Lighting | Light-emitting diodes | Colour 1: neutral white, colour 2: UV ≈ 420 nm |

The sample of the images for ten classes of paper for recycling is shown in Figure 2.5 below:



Figure 2.5: Sample images of ten classes (Gottschling & Schabel, 2016)

Image segmentation was done greyscale transformation, global thresholding, area opening and flood filling of holes. Feature extraction was done for 26 features grouped in weight, shape, colour, texture and amount of optical brightness. As the setup cannot be screened from the surrounding light, only robust features against inconsistencies in the lighting condition were chosen.

The weight of each piece of paper was calculated by the Equation 2.1

$$\rho_A = \frac{m}{A} \quad (2.1)$$

Where A is total area, m is the total mass of a piece of paper, and ρ_A is the mass per unit area.

The aspect ratio was given by Equation 2.2:

$$e = \frac{b}{t} \quad (2.2)$$

Where b is width, and t is the length of a small area enclosed in the paper piece.

The hue and saturation of the unprinted templates of newspapers, white paper and corrugated board lie in the typical ranges so the classes can be distinguished. To perform that, they chose four paper colour regions: brown, grey 2, grey 1 and white. The borders are listed in the Table below:

Table 2.2: Borders of paper color regions (Gottschling & Schabel, 2016)

| <i>Name</i> | <i>Abbreviation</i> | <i>Hue in °</i> | <i>Saturation in %</i> |
|-------------|---------------------|-----------------|------------------------|
| Brown | b | 29.0 to 37.5 | 59.0 to 70.0 |
| Grey 2 | g2 | 36.0 to 42.5 | 42.5 to 57.0 |
| Grey 1 | g1 | 42.5 to 48.0 | 42.5 to 50.0 |
| White | w | 42.0 to 50.0 | 33.0 to 42.5 |

To calculate the four novel colour features, the image was subdivided into square windows shown in Figure 2.6 below.

The calculations for the hue and standard deviation were done by taking the standard deviation of hue and the standard deviation of standard deviation.

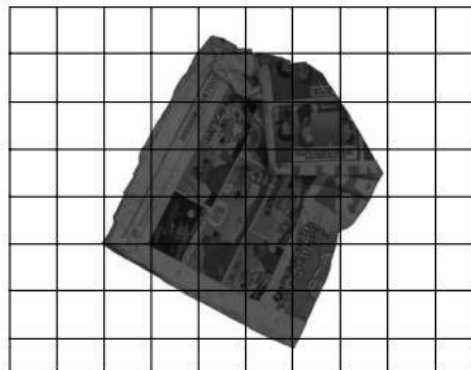


Figure 2.6: Subdivision of an image into square windows (Gottschling & Schabel, 2016)

The texture features were extracted after transforming the RGB image to a greyscale image. The luminance Y in the NTSC color space was chosen as intensity. After all feature's extractions, the feature data was transformed with the normalization parameters for each feature j .

$$z_j = \frac{t_j - \bar{x}_j}{s_j} \quad (2.3)$$

Where z_j is a transformed data point, t_j is original data point, \bar{x}_j represents arithmetic mean of the dataset for training and testing, s_j is standard deviation of the dataset for training and testing

Six hundred ninety pieces of each class were randomly chosen for training and testing. For all features and all classes, Tukey boxplots were calculated and evaluated. Pearson's correlation was computer among the feature to determine the correlation with other features.

50% of the dataset was chosen for training. The first five- stage classifiers with their specification are listed in Table 2.3. below:

**Table 2.3: Specification of first stage classifiers
(Gottschling & Schabel, 2016)**

| <i>Number</i> | <i>Classifier</i> | <i>Specifications</i> |
|---------------|-----------------------------|--|
| 1 | <i>k</i> -nearest-neighbour | $k = 5$ |
| 2 | Quadratic discriminant | - |
| 3 | Decision tree | Pruned to the largest pruning level that achieves a value of cross-validation classification error (E) within the standard error of E of the minimum error |
| 4 | Neural network | Two-layer feedforward network, with sigmoid transfer functions; number of hidden neurons: 20; training set size: 70%, validation set size: 30% |
| 5 | Support vector machine | Multiclass: one-versus-the-rest; kernel function: dot product; method to find the separating hyperplane: least squares |

The remaining 50% of the dataset was used for testing. Their findings are shown in the figures below:

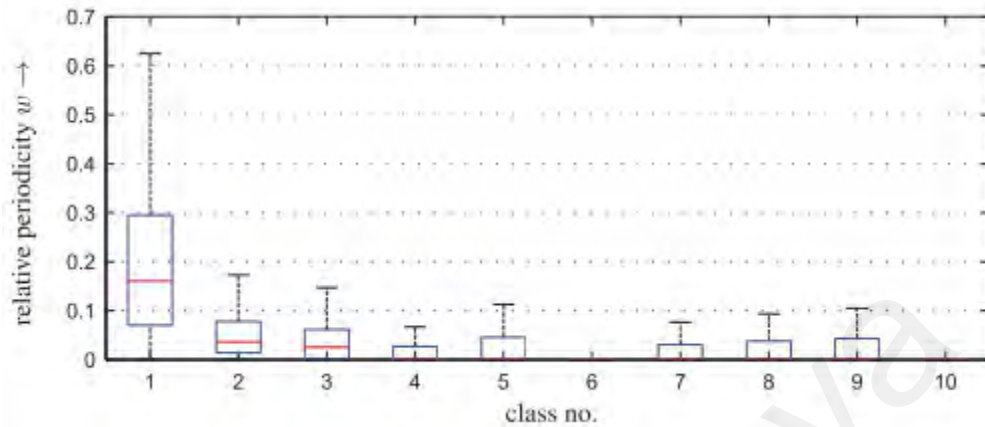


Figure 2.7: Tukey boxplot for the relative periodicity without outliers (Gottschling & Schabel, 2016)

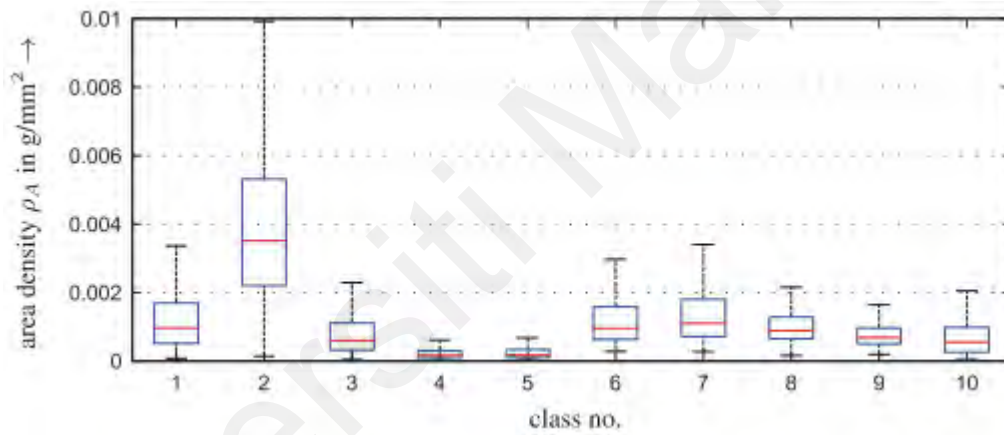


Figure 2.8: Tukey boxplot for the area density without outliers (Gottschling & Schabel, 2016)

All features can distinguish between some classes or part of classes. However, the distribution of some classes largely overlaps. The classification success rates of the primary classification system for all classes are listed in Table 2.5 below:

**Table 2.5: Success rates of the system with all classes in %
(Gottschling & Schabel, 2016)**

| Class no. | Classifier no. | | | | | Combination |
|-----------|----------------|----|----|----|----|-------------|
| | 1 | 2 | 3 | 4 | 5 | |
| 1 | 95 | 93 | 76 | 92 | 54 | 96 |
| 2 | 88 | 88 | 84 | 84 | 51 | 88 |
| 3 | 79 | 86 | 72 | 74 | 22 | 84 |
| 4 | 85 | 93 | 83 | 86 | 35 | 90 |
| 5 | 75 | 87 | 75 | 80 | 30 | 82 |
| 6 | 94 | 91 | 83 | 89 | 36 | 91 |
| 7 | 42 | 47 | 51 | 52 | 48 | 51 |
| 8 | 34 | 26 | 36 | 31 | 17 | 32 |
| 9 | 39 | 43 | 63 | 54 | 58 | 58 |
| 10 | 35 | 17 | 33 | 18 | 80 | 32 |

The success rates are relatively high for classes 1 to 6 (over 80%), but it was relatively low (under 50%) for the remaining classes. The modified system results for classes 1 to 6 are shown in Table 2.4 below:

**Table 2.4: Success rate of the modified system in %
(Gottschling & Schabel, 2016)**

| Class no. | Classifier no. | | | | | Combination |
|-----------|----------------|----|----|----|-----|-------------|
| | 1 | 2 | 3 | 4 | 5 | |
| 1 | 97 | 95 | 86 | 91 | 81 | 96 |
| 2 | 93 | 95 | 88 | 93 | 90 | 94 |
| 3 | 98 | 97 | 97 | 97 | 90 | 98 |
| 4 | 97 | 98 | 99 | 99 | 100 | 98 |
| 5 | 91 | 92 | 93 | 94 | 93 | 94 |
| 6 | 99 | 98 | 97 | 98 | 99 | 99 |

It was concluded that out of 26 features that are robust against light conditions, ten are novel: the relative scores of colors brown, grey 2, grey 1 and white, the mean of the standard deviation of the saturation, the standard deviation of the saturation, the mean of the standard deviation of the hue, the standard deviation of the hue, the relative periodicity and the amount of the optical brighteners. Seven are not novel and not reported in pattern recognition until now: the total mass, area density,

length, width, aspect ratio, smoothness, and uniformity. Feature assessment showed that all features have the discriminative capability, but it is often limited to certain classes. The modified system for six classes showed a success rate between 94% and 100%. Improvement can be achieved by optimizing the classifiers or by implementing more sophisticated classifiers, for example, a fuzzy inference system.

(Doak et al., 2006) patented a system that uses light sources of multiple wavelengths and calculated the following features: color, intensity, and gloss. It identified white papers, newspapers, magazines, and brown cardboard.

2.3.2 Plastic Sorting

An artificial intelligent plastic bottle classification system is proposed, developed, and tested in this work. It is attempted to classify bottles based on their chemical composition and colour. Near infrared (NIR) reflectance measurements are used to determine the composition class of a bottle. To detect bottle color, a charged coupled system (CCD) camera with a combination of quadratic discriminant analysis (QDA) and tree classifier was used. The results showed that the reflective NIR spectrum's dip wavelength and average values could be used to differentiate between chemical compositions. This resulted in a classification accuracy of 94.14 percent. The proposed method achieves 92 percent colour classification accuracy for transparent bottles and 96 percent for opaque bottles. The combined system's aggregate classification accuracy was 83.48 percent (Tachwali et al., 2007).

(Anzano et al., 2006) used statistical correlation analysis, a compact laser-induced plasma spectrometer had been designed for fast, reliable categorization of distinct groups of plastic materials. Data gathering and data processing functions were combined in a software package. Linear and non-parametric (rank) correlations were used to classify spectral data, and the results were nearly identical. The technique's reliability was proved by the 90–99 percent accurate

identification of practically all polymers tested.

Different sorting procedures for segregating plastic materials were investigated (Dodbiba & Fujita, 2004). The focus of the review was on non-sensor-based design, development, and testing of wet and dry separating/sorting approaches.

Recycling discarded plastic bottles is an essential step toward protecting the environment and conserving resources. Bottles in different colours usually have different recycling values. The classification of plastic bottles during recycling based on image recognition is an effective method, with location and colour recognition as main technologies. To distinguish the plastic bottles on the conveyor belt, their location relationships are first classified as disjoint, adjacent, or overlapping. The ratio of concave and convex area based on their image easily identifies the disjoint ones. To distinguish their position relationships, a hybrid method called distance transformation and threshold segmentation is proposed for adjacent and overlapping bottles. If the adjacent bottles have been identified, a concave point scan based on a convex hull will be used to further distinguish the adjacent recycled bottles. The colour of both the disjoint and neighbouring bottles is then identified since it is too complicated and difficult to recognise and differentiate the colour of the overlapping bottles. In terms of colour identification, the colours of recycled bottles are classified into seven groups throughout the sorting process. Since there may be a bottle cap and a label on the top and middle of the bottle, respectively, resulting in incorrect identification, colour features of the bottom portion are used to reflect the one of the recycled bottles. The ReliefF algorithm is used to select colour features of recycled bottles, which are then identified using the support vector machine (SVM) algorithm. The effect of training sample size on classification model is investigated, and experimental results show that colour recognition accuracy of recycled bottles reaches 94.7 percent. However, when the number of samples approached 1400, the stability and precision of the identification tend to saturate (Adedeji & Wang, 2019).

First and foremost, photos of the plastic bottles were taken, and several preprocessing measures were completed. The first step in preprocessing is to separate the plastic region of a bottle from the context. The morphological image operations are then carried out. Edge detection, noise reduction, hole removal, image enhancement, and image segmentation are examples of these operations. These morpho-logical operations can be broadly described as combinations of erosion and dilation. Since it provides a global solution to a classification problem, Support Vector Machine (SVM) is chosen to complete the classification task. The decision process consists of five separate feature extraction methods, including Principal Component Analysis (PCA), Kernel PCA (KPCA), Fisher's Linear Discriminant Analysis (FLDA), Singular Value Decomposition (SVD), and Laplacian Eigenmaps (LEMAP), and is implemented using a simple experimental setup with a camera and homogeneous backlighting. It can automatically identify plastic bottle forms with a recognition accuracy of about 90% (Özkan et al., 2015).

In Raman spectroscopy (Tsuchida et al., 2009), molecular vibration is observed at each peak that gives information about the molecule...e structure plastic types are identified accordingly. Since the pre-processed dataset gives many peaks, this method is more efficient when used on a pre-processed dataset. The system setup is shown in Figure 2.9.

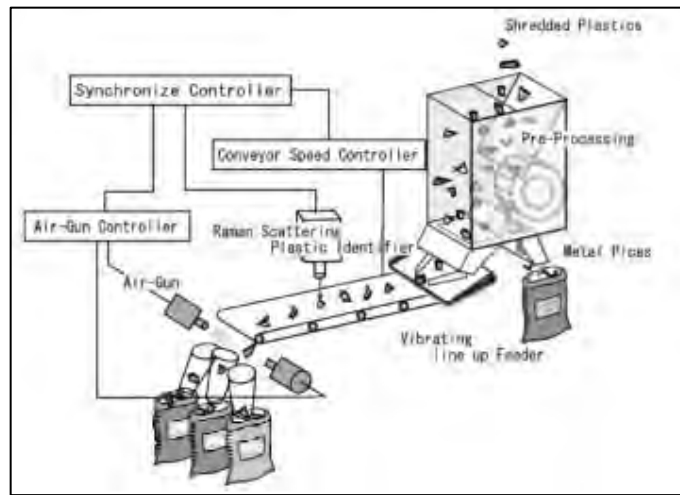


Figure 2.9: Scheme of the plastic sorting system with Raman Spectroscopy (Tsuchida et al., 2009)

The post-consumer plastic went through pre-processing in the above system, which removed metals, wire, labels, and similar contaminations. Then the plastic went under a spectrometer for analysis. The last stage consists of an air gun used to sort out the known pieces of plastics.

They mentioned that Raman spectroscopy has more advantages like no reference signal is required, the signal to noise ratios (SNR) is easily achieved by pumping laser and surface conditions. Additionally, H₂O and CO₂ in the air have fewer effects.

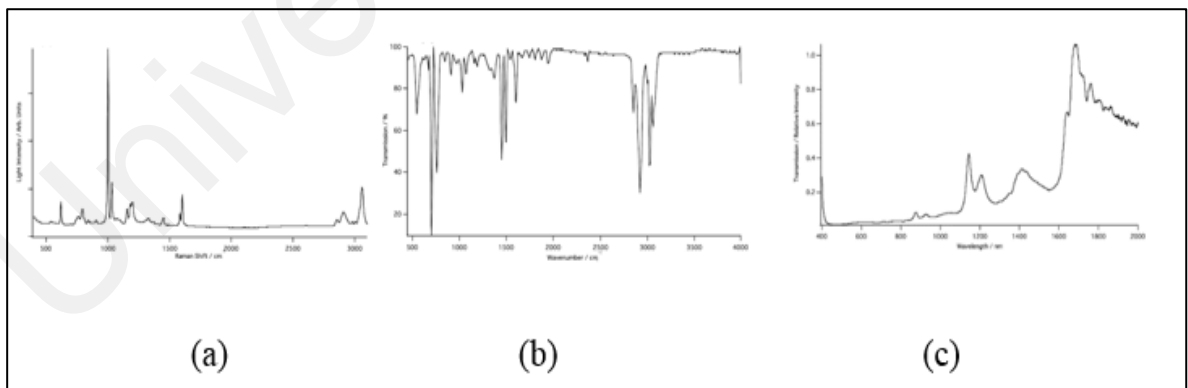


Figure 2.10: Spectra of polystyrene in (a) Raman, (b) IR and (c) NIR (Tsuchida et al., 2009)

Raman spectroscopy would be able to improve the purity and sorting speed as compare to NIR. As shown in Fig 2.10 NIR spectrum consist of complex harmonics and degradation of SNR because of broad peaks. Symmetric vibration such as ring breezing in benzene structure is known as active in Raman but inactive in IR (Figure 2.10 (a) and (b)). They collected 125 spectra from 120 test pieces of post-consumer plastics. They categorised them into four groups (i.e. PP, PS, ABS and unknown).

Raman spectra use molecular vibration known as normal vibration, which produces peaks, which provide molecular structure information, each of which is unique. Figure 2.11 shows the data processing flow of the experiment.

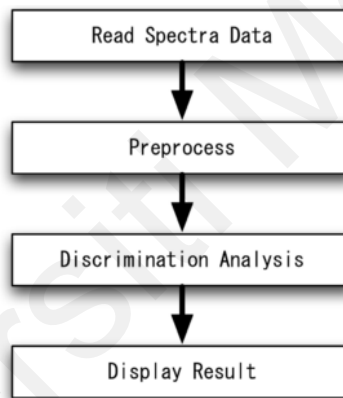


Figure 2.11: Data processing flow (Tsuchida et al., 2009)

In Figure 2.12, the robustness of Roman spectra of PP, PS and ABS with characteristic peaks with good SNR is shown, with the measurement time of 6ms.

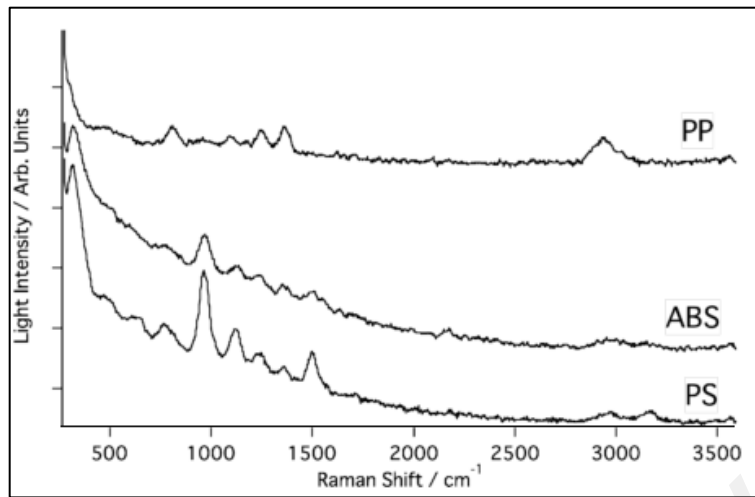


Figure 2.12: Raman spectra of PP, ABS and PS measure in 6m (Tsuchida et al., 2009)

The above spectra were obtained after several improvements in the spectrometer as a pre-processing method was applied for the accuracy of the spectrum analysis. The result was improved by 94%. Figure 2.13 shows the accuracy dependency on the pre-processing method.

Spectra data was folded up to equal widths of 127 to 8 channels each. The accuracy was highest when 16 data channels were added and average.

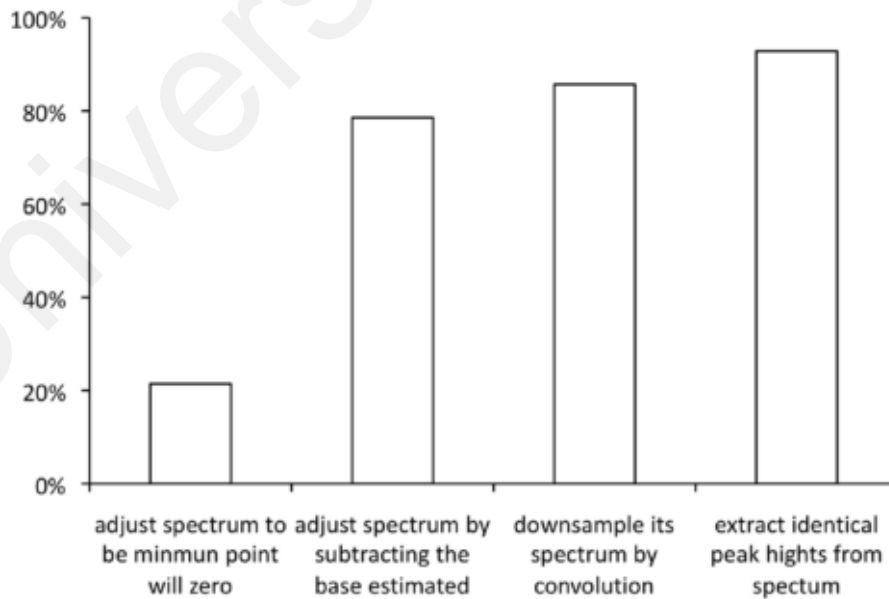


Figure 2.13: Accuracy dependence on pre-process method (Tsuchida et al., 2009)

Discrimination analysis was used for calculation for the selected target. Figure 2.14 presents Raman spectra for the resulting value of the minimum (a) and the maximum (b) in a histogram.

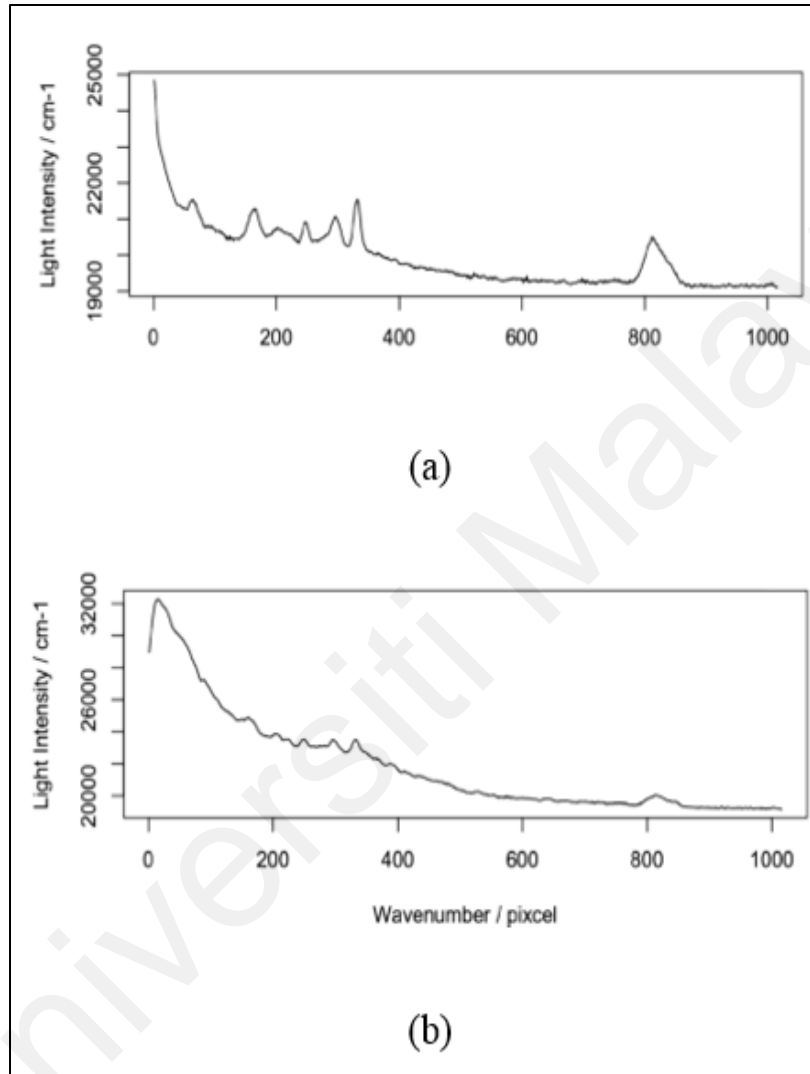


Figure 2.14: Difference of typical Raman spectrum
(a) when the calculated value is less than zero,
(b) when calculated value becomes highest (Tsuchida et al., 2009)

The high-speed Raman spectra system developed in their work could measure the appropriate SNR spectrum and identify plastics with multivariate analysis in less, i.e., 1.5 milliseconds.

(Edward & Bruno, 2000) research paper provided information on available sorting methods of plastics. He divided plastic sorting into micro sorting and macro sorting. Micro sorting is the sorting of chopped plastic, and sorting of whole bottles or containers is macro sorting. Figure 2.15 shows the technologies and methods are being used for macro sorting and micro sorting.

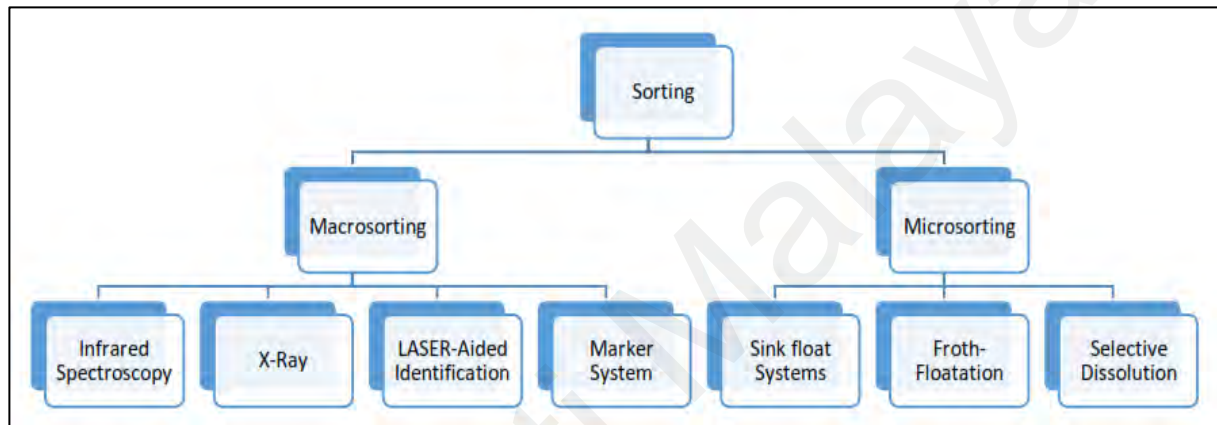


Figure 2.15: Sorting technologies for Macro-sorting and Micro-sorting (Edward & Bruno, 2000)

Near-infrared spectroscopy involves irradiating the unsorted and unidentified plastic using a near-infrared wave with a wavelength of 600-2500 nm. In this method, infrared light hit and reflect from the target plastic resin. Each resin type has different characteristics through which can be measured on an infrared absorption band. The X-Ray sorting technique uses the study of the spectrum of reflected waves from unknown plastics. This technology is mainly applied for the sorting of PVC.

LASER-Aided system uses the shining of the emitted laser beam on the different plastic material surface. Then identify the material by analysing the response of the reflected beam. The

marker system method involves readily detectable marking on either the resin or container. Implementing this system requires cooperation among resin manufacturers and recyclers.

He concluded that each sorting method could be used and provide promising results. Nevertheless, the ideal system would be a combination of all methods available, and more studies need to be done for the ideal process. Future studies should focus more on the systems' efficiency, and research is required to test the newer technologies in building large-scale systems.

(Tachwali et al., 2007) proposed an artificial intelligent system for plastic bottle sorting. The system used near-infrared (NIR) reflectance measurement and charged couple device (CCD) camera with tree classifiers and quadratic discriminant analysis (QDA). The former was used to identify bottle composition class and later was used to detect bottle color. NIR spectrum produced 94.14% classification accuracy, and QDA produced 96% color classification accuracy. The accuracy of the combined system was 83.48%.

2.4 Sorting Techniques

2.4.1 Image Processing

Sorting waste packaging material for recycling is very important for industry. (Özkan et al., 2015) proposed an automated system for sorting plastic bottles and selected only three types due to their higher existence ratio: PET, HDPE, and PP. They use five different feature extraction methods for decision-making, which were Principal Component Analysis (PCA), Kernel PCA (KPCA), Fisher's Linear Discriminant Analysis (FLDA), Singular Value Decomposition (SVD), and Laplacian Eigenmaps (LEMAP). Their experimental setup is shown in Figure 2.16. The system's sorting capacity is 750 kg/h, and the sorting belt speed is 0.25 m/s. The web camera was placed on one side in order to take photos. All the steps taken are shown in Figure 2.17.



Figure 2.16: Prototype of sorting system (Özkan et al., 2015)

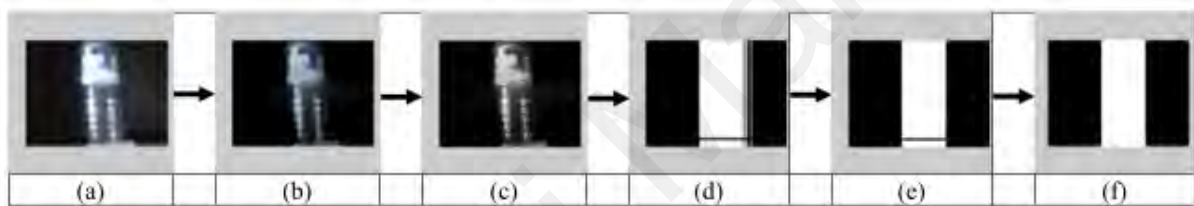


Figure 2.17: The pre-processing steps for structure identification of a plastic bottle (Özkan et al., 2015)

They used detection algorithms to extract images from the background. If Figure 2.17. (d) The image's location was identified using Otsu's thresholding method, then the opening and closing morphological image operators were performed to subtract the image from its background. The details and redundancies (see right side of Figure 2.17(d)) were filtered using morphological opening (erosion followed by dilation), then closing operation (dilation followed by erosion) was performed as given in Figure 2.17(e). The extracted area from the plastic bottle is given in image Figure 2.17(f).

The data set consist of three different bottle types (PET, HDPE, and PP) images, and each class had 30 images for each type. The image background information was eliminated using various steps mentioned above. Then image vector for each image was obtained with the dimension of

(1x1000). The dimension of the image was reduced before classification scheme to obtain a lower-dimensional feature space. PCA, KPCA, FLDA, and SVD were applied to obtain the image vectors whose dimension was (1 x 100). The experiments performed are shown in Figure 2.18.

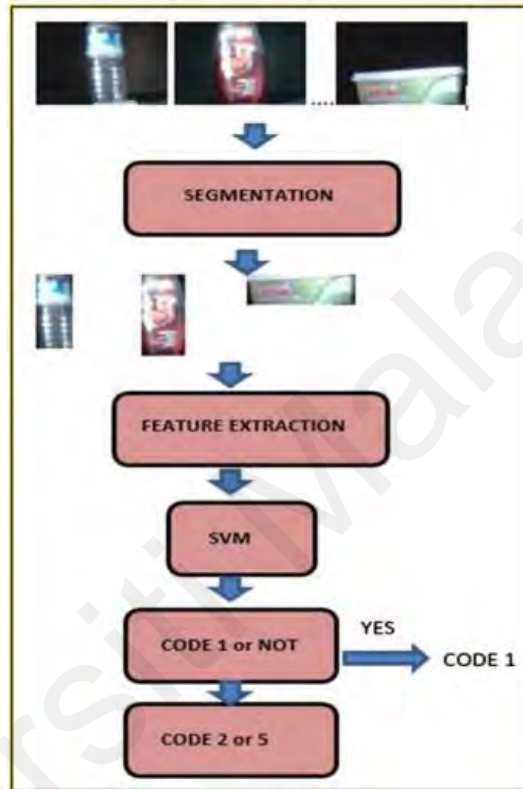


Figure 2.18: The experiment stages of the recognition scenario (Özkan et al., 2015)

SVM was used for the classification task. The majority voting algorithm was used in the classification as well. The classification decision was obtained from five extraction methods, and then most voted class was accepted. The classification framework consisted of two- stages. The first stage uses SVM to classify PET and non-PET. In the second stage, non-PET bottles were classified as HPDE or PP. The classification framework and accuracy are shown in Table 2.6. Moreover, the confusion matrix in Table 2.7 shows the classification performance.

The values in the confusion matrix show the number of correct/incorrect classified data. Each column shows the predicted class, and each row shows the actual class. All correct results are in diagonal of the matrix. The 1/6 of the dataset was used as testing and 5/6 for training to test all plastic photos, from Table 2.7. Fig.2.19 shows some misclassified samples of plastic bottles of different types.

The classification accuracy is shown in Table 2.6. It is observed that LEMAP shows the worst recognition performance, but KPCA proved to be the best among the five feature extraction methods.

Table 2.6: Classification rate (%) of plastic types (Özkan et al., 2015)

| | PCA | KPCA | LDA | LEMAP | SVD | Majority Voting classifier combination |
|----------------|-----|------|-----|-------|-----|--|
| PET | 70 | 77 | 80 | 57 | 80 | 87 |
| HPDE | 77 | 80 | 87 | 63 | 83 | 90 |
| PP | 60 | 83 | 70 | 73 | 67 | 80 |
| Average | 69 | 80 | 79 | 64 | 77 | 88 |

Table 2.7: Confusion matrix for all classes (Özkan et al., 2015)

| | PET | HPDE | PP |
|-------------|-----|------|----|
| PET | 26 | 3 | 1 |
| HPDE | 1 | 27 | 2 |
| PP | 1 | 5 | 24 |



Figure 2.19: A few samples of some correctly and incorrectly classified plastic objects (Özkan et al., 2015)

The first stage of the classification into PET and non-PET experimental results are shown in Figure. 2.20. The recognition rates were computed using SVM. One-third database is PET samples (1-30), and the rest of the database consists of non-PET samples (31-90). At this stage, the LDA feature extraction method performs best among all other methods. Another two-class classification was performed in the second stage to distinguish HDPE or PP from non-PET type plastic bottles. The recognition outcomes are shown in Figure 2.21. The KPCA method exhibits the best results as compared to other methods at the second stage. The non-PET samples (31-60) and (61-90) represent HDPE and PP types of plastic bottles, respectively.

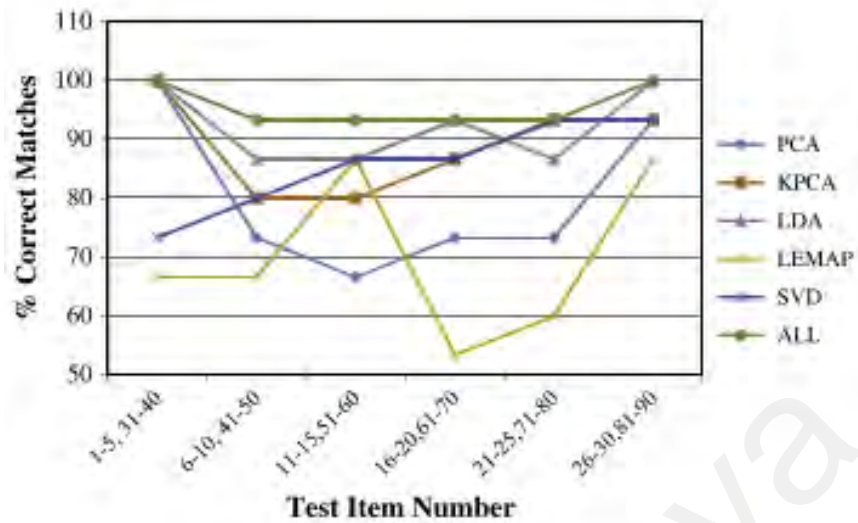


Figure 2.20: Experiments results on the classification of the PET and non-PET plastic bottles (Özkan et al., 2015)

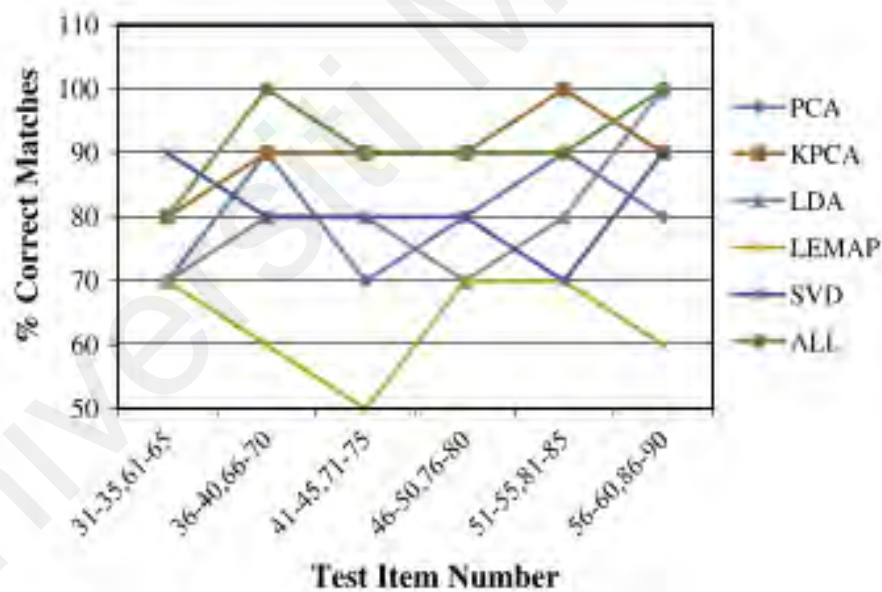


Figure 2.21: Experimental results on the classification of the HDPE and PP plastic bottles(Özkan et al., 2015)

The main possible problem for online implementation was that bottles might be wrinkled, so that morphological image operation was not conducted properly. Another problem is that a plastic bottle may have cut or damaged, confusing the PET and non-PET classification stage. The solution might be to place the smoothed bottle on the conveyor belt.

(Huibin Yang & Yan Juan, 2015) Their research paper provided an industrial sorting system based on robot vision technology, introducing image processing and algorithm simulation using MATLAB. The workpiece's regular geometry was done by setting up the MATLAB image processing library via C#. By analyzing and calibrating the camera, processing many images, they could resolve a standard workpiece's identification problem with different colors. The system structure is shown in Figure 2.22.

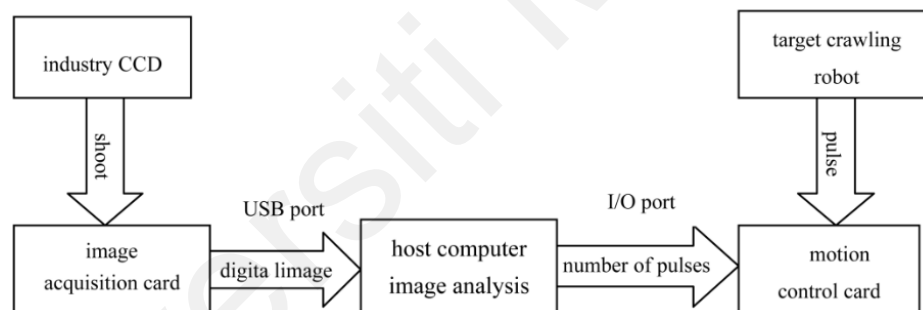


Figure 2.22: Piece sorting based on a machine vision (Huibin Yang & Yan Juan, 2015)

Their hardware consisted of an automated three-axis motion platform, camera platforms, PC, and motion control unit. Because of the stable environment and laboratory, they use the Direct Linear Method for camera calibration. To detect the workpiece, they use image segmentation and edge detection method. For sorting operation, the workpieces needed to be identified for positioning, the general centroid coordinates were used to describe the workpiece's position information.

The system was able to recognise square, rectangle, circle, and any other regular shape workpiece. Researchers wrote the program in C#, and the result is shown in Figure 2.23.

To identify the workpiece and reach the top of the target, the number of pulses is required to send to motion control card, which controls the robot's motors and achieves the sorting process. The system identifies the workpiece with a correct rate of 100%, and the error of the target location is less than 5mm.

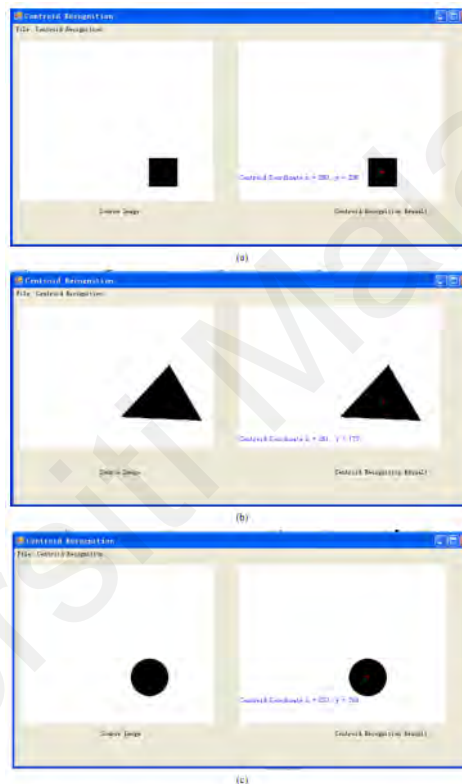


Figure 2.23: Rule workpiece centroid recognition (Huibin Yang & Yan Juan, 2015)

(Jiao & Sun, 2016) developed a highly accurate real-time sorting algorithm based on RGB color space and image processing, especially for white and grey recycled particles shown in Figure 2.24 – 2.26. That algorithm used related addition, multiplication, and comparison operations of corresponding pixels of R, G, and B. They presented two theorems, first that the value of $(R+G+B)$, which is the summation of R, G, and B of every image in a given plane, can be expressed as

$R+G+B=3m$ and secondly, the radius of the circle approximately can be: $\text{radius} = \sqrt{6/12} [(R_{\max} - R_{\min}) + (G_{\max} - G_{\min}) + (B_{\max} - B_{\min})]$. The maximum distance r from each point of the qualified particle space “mallet” to the space RGB coordinate origin is $r = \sqrt{(3m^2 + (\text{radius})^2)}$ and distance from the renewable particle image:

$D = \sqrt{(R^2 + G^2 + B^2)}$. Moreover, if $D \leq r$, then the particle being detected is a qualified particle.

If $D > r$, the actual particle belongs to the second or this Harmonia particle. They proposed the following algorithm steps:

- a. Capture the image point of the particle to be picked with a CCD camera.
- b. Calculate the sum of R, G and B coordinates $3m$ and D .
- c. Compared $3m$ with the minimum, if $3m < \min$, it is black particles.
- d. Otherwise, compare $D^2 \leq r^2$, it is a qualified particle
- e. On the contrary, it can be red, blue, or other color or white poor quality color.



Figure 2.24: Qualified white regenerated parties (Jiao & Sun, 2016)



Figure 2.25: Regenerate particles mixed with different color particles (Jiao & Sun, 2016)

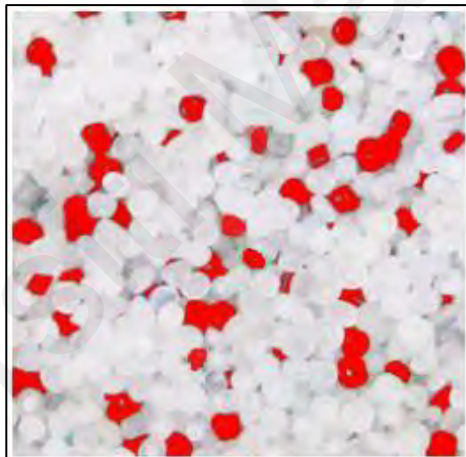


Figure 2.26: Sorting result (Jiao & Sun, 2016)

The algorithm can effectively pick the Harmonia particles from the mixed white particles, and the algorithm sorting rate was 95% and can be applied to other related projects.

(Sofu et al., 2016) proposed a real-time quality inspection system for automatic apple sorting. Three types of apples, Golden, Starking Delicious, and Granny Smith, were sorted in color, size, and weight. They used two identical industrial cameras on a roller conveyor, and four images of any apple rolling on conveyor were processed in image processing software in 0.52 sec. The system was able to sort an averagely of 15 apples per second using two channels. The whole system

was controlled by PLC, which includes actuators, conveyors, and bowls. Their machine achieved sorting of 432 apples/day with an accuracy of 79%.

The roller conveyor was used to take at least four images of each apple. The enclosed cabin was designed to house the camera and lighting system. In this way, homogeneous illumination was provided for successful apple sorting. The machine vision system obtains the visual features of the apples. The brush system moved the apples from the roller conveyor to the transporter conveyor.

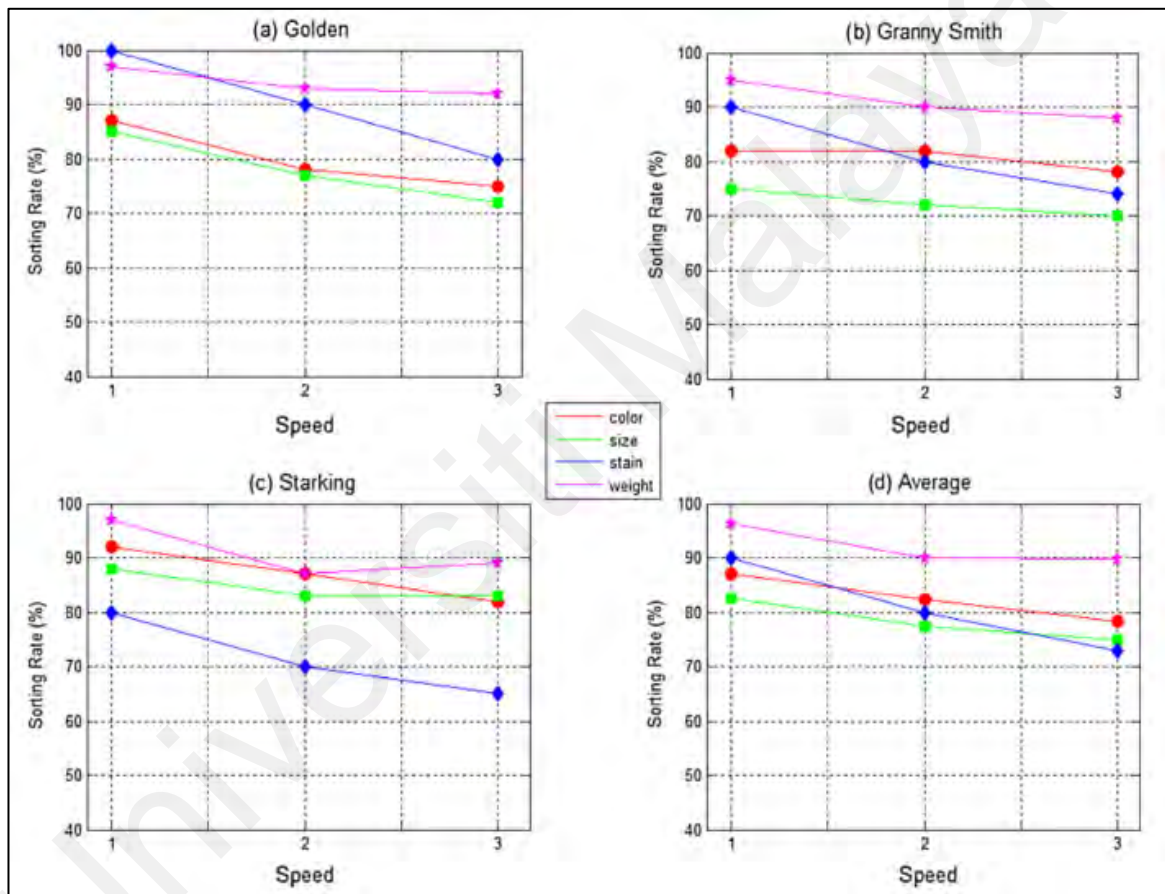


Figure 2.27: Sorting rates of three apple cultivars and their average values (Sofu et al., 2016)

The load cells measured the weight of apples. The bowl and its triggering systems were used for successful sorting. The PLC controlled all the actuators, conveyors, and bowls.

The captured and processed images displayed the color, size, area, and defective regions of the apples. The C4.5 classifier, a rule-based method, was used to sort apples according to their

features. In experimental studies, although Golden Delicious, Granny Smith, and Starking Delicious were evaluated, other cultivars of apple can also be evaluated in this machine. The result of the sorting rate of three apples cultivars and their average values are shown in Figure: 2.27.

(Duan et al., 2007) proposed a method for inspection of beer bottles based on vision technology and used histogram of the edge points is applied for real-time determination of inspection area. The algorithm worked in three steps, (i) Mark and determination of inspection area, (ii) Inspection of bottle wall and bottle bottom, and (iii) Inspection of bottle finish.

The first step used a histogram of edge points to locate the inspection area, then edge points from bottom shoulder to bottle finish were found according to a carefully selected threshold. The same algorithm was used to detect the center of the image. The algorithm used the statistic to delete distributive disturbance with large values.

The second step included pre-processing of the inspection area and then the transformation of an image to a binary image, which enabled to detection of more defective areas. The rising and falling edge points of the horizontal and vertical directions were obtained. From these edges, statistical information was obtained. Furthermore, finally, from the threshold value and size of the component, the defected area was confirmed.

The third step used two neural networks, low-level inspection, and high-level judgment as shown in figures below. The former method inspects the serial parts of the finish area. 40 samples were taken for training than used for high-level judgment.

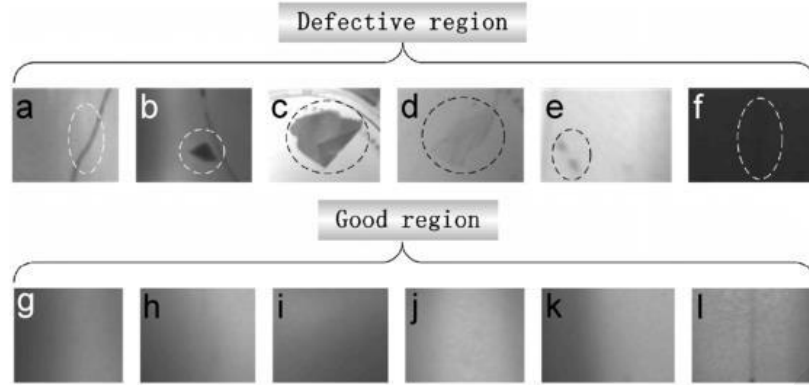


Figure 2.28: Some defect in bottle wall and bottom (Duan et al., 2007)

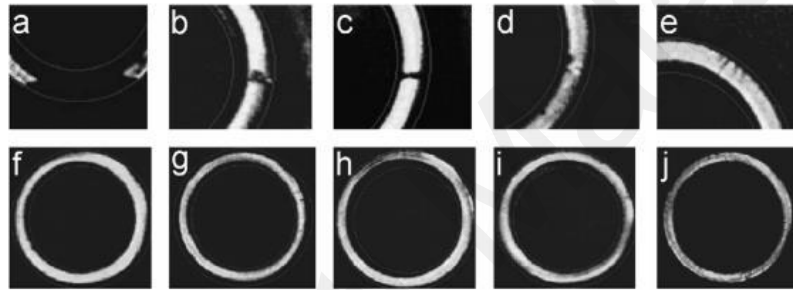


Figure 2.29: Some typical finish images (Duan et al., 2007)

The results obtained are shown in tables below.

Table 2.8: Inspection results of defective bottle walls and bottoms (Duan et al., 2007)

| Samples | Fig 28a | Fig 28b | Fig 28c | Fig 28d | Fig 28e | Fig 28f |
|-----------------------------|---------|---------|---------|---------|---------|---------|
| Correct inspection rate (%) | 100 | 100 | 100 | 98 | 96 | 90 |

Table 2.9: Inspection results of good bottle walls and bottoms (Duan et al., 2007)

| Samples | Fig 28g | Fig 28h | Fig 28i | Fig 28j | Fig 28k | Fig 28l |
|-----------------------------|---------|---------|---------|---------|---------|---------|
| Correct inspection rate (%) | 100 | 100 | 100 | 98 | 96 | 90 |

Table 2.10: Inspection results of defective finish (Duan et al., 2007)

| Defect Samples | Fig 29a | Fig 29b | Fig 29c | Fig 29d | Fig 29e |
|-----------------------|----------------|----------------|----------------|----------------|----------------|
| Correct inspection | 100 | 100 | 100 | 98 | 96 |

Table 2.11: Inspection results of good finish (Duan et al., 2007)

| Defect Samples | Fig 29f | Fig 29g | Fig 29h | Fig 29i | Fig 29j |
|-----------------------|----------------|----------------|----------------|----------------|----------------|
| Correct inspection | 100 | 100 | 96 | 94 | 92 |

Universiti Malaysia

2.5 Research Gap

Table 2.12: Research Gap Analysis

| No | Type of Material Sorted | Sorting Methods/Techniques | Outcome | Future Scope | Reference Paper/ Material |
|----|--|--|---|---|---|
| 1 | Glass, Plastic, Paper, and Metal | Electronic Controller, LDR and LASER Sensors | i. System is good example of good sorting mechanism. | i. System can be used to sort more material. ii. Response time can be increased. iii. On large scale manufacturing, the price can be cheaper. iv. Not intelligent enough to sort more types of material. | (Md Mahmudul Hasan Russel et al., 2013) |
| 2 | Paper | Distinguish 10 classes, and 26 features. | i. System distinguishes between 10 classes of paper and success rate of 94% to 100% was reported. | i. Improvement can be achieved by optimizing the classifiers or by implementing more sophisticated classifiers, for example a fuzzy inference system | (Gottschling & Schabel, 2016) |
| 3 | Paper, Newspapers, Magazines and Brown Cardboard | Light sources of different wavelength | i. Each category of the paper was uniquely identified | i. The incoming stream of papers can be sort in more than two fractions. ii. Not intelligent enough to sort more types of material. | (Doak et al., 2006) |

Table 2.12: Research Gap Analysis (Continued)

| No | Type of Material Sorted | Sorting Methods/Techniques | Outcome | Future Scope | Reference Paper/ Material |
|----|-----------------------------------|---|---|---|---------------------------|
| 4 | Plastic (PP, PS, ABS and unknown) | Raman Spectroscopy | i. Identify plastics with multivariate analysis in less as 1.5 milliseconds | i. Not suitable for paper sorting. | (Tsuchida et al., 2009) |
| 5 | Plastic | Review Paper on different methods | i. Each sorting method can be used and provide promising results | i. The future studies should focus more on the efficiency of the systems and research is required to test the newer technologies in building large scale systems | (Edward & Bruno, 2000) |
| 6 | Plastic Bottles | i. NIR and CCD ii. Tree classifier iii. Quadratic Discriminant Analysis | i. 92% result was achieved for clear bottles while 96% for opaque bottles. The overall combined accuracy of system was 83.48 %. | i. Develop further too support multiple bottle classification. ii. Shape classification to separate deformed plastic bottles. iii. Can be used for non-bottled shaped plastic | (Tachwali et al., 2007) |

Table 2.12: Research Gap Analysis (Continued)

| No | Type of Material Sorted | Sorting Methods/Techniques | Outcome | Future Scope | Reference Paper/ Material |
|----|--------------------------------|---|--|---|---------------------------|
| 7 | Plastic Bottles | <ul style="list-style-type: none"> i. Principal Component Analysis (PCA), ii. Kernel PCA (KPCA), iii. Fisher's Linear Discriminant Analysis (FLDA), iv. Singular Value Decomposition (SVD) v. Laplacian Eigenmaps (LEMAP). | <ul style="list-style-type: none"> i. PET and non-PET samples LDA performs best. ii. HDPE and PP samples KPCA performs best. | <ul style="list-style-type: none"> i. Possible problem for online implementation was that bottles may be wrinkled. ii. Another problem is that a plastic bottle may have cut or damaged which can cause confusion during PET and non-PET. | (Tachwali et al., 2007) |
| 8 | Mixed garbage of 40 categories | Raspberry Pi 4B was utilized as the master board for the hardware system and GNet model for garbage classification based on transfer learning and the improved MobileNetV3 model was proposed. | The proposed classification system's prediction accuracy was 92.62% at 0.63 s efficiency. | The object detection system will be utilized to recognize multiple types of garbage simultaneously. | (Fu et al., 2021) |

Table 2.12: Research Gap Analysis (Continued)

| No | Type of Material Sorted | Sorting Methods/Techniques | Outcome | Future Scope | Reference Paper/ Material |
|----|---|---|---|---|----------------------------|
| 9 | Garbage segregation and monitoring for the bins | The key microcontroller NodeMCU detects the amount of waste in the bin using an ultrasonic sensor as a level detector. Other sensors like infrared, moisture, servo motor, and Global system for mobile (GSM), GPS, will provide real-time information. | The proposed system detects the level of garbage in the bins and provide real time data for the waste management and send data to society office. | The proposed system goes under a useful step towards cleanliness. | (Lachi Reddy et al., 2021) |
| 10 | Municipal garbage waste | This study proposed garbage classification system based on the Mask Scoring RCNN algorithm. | Hazardous Garbage: 58.9% Kitchen Garbage: 65.5% Recyclable Garbage: 68.8% Other Garbage: 64.8% Average accuracy: 65.8% | More comprehensive data set can provide improved results. | (Li et al., 2020) |

Table 2.12: Research Gap Analysis (Continued)

| No | Type of Material Sorted | Sorting Methods/Techniques | Outcome | Future Scope | Reference Paper/ Material |
|-----------|---|---|---|---|----------------------------------|
| 11 | Dry garbage, wet garbage, hazardous garbage and recyclable garbage. | They created intelligent classification garbage bins and performed the automatic classification by using core controller composed of camera, input/output and communication module. | Image recognition accuracy was 76.92% and the classification accuracy they reported was 92.31%. | The classification accuracy can be improved further with the collection of more dataset of the garbage. | (D et al., 2021) |

Based on the summary above, the methods from neural networks (Duan et al., 2007) and classification methods (Doak et al., 2006), tree classifier, and quadratic discriminant analysis (Tachwali et al., 2007) with optical sensors and controller (Md Mahmudul Hasan Russel et al., 2013) with image processing software capability (Huibin Yang & Yan Juan, 2015) and (Özkan et al., 2015) can provide a promising results for paper and plastic sorting for waste management using artificial intelligence.

In a nutshell, from the research gap analysis, the artificial intelligent network can be developed by using image processing techniques with the powerful hardware and software tools to build a system that can sort multiple waste for the recycling management industry.

CHAPTER 3: METHODOLOGY

3.1 Introduction

The proposed Automated Sorting Conveyor (ASC) for garbage consist of several modules: image acquisition, feature extraction, classification and automatic sorting through conveyor and electro-pneumatic separators. Figure 3.1 shows the overview of the proposed system.

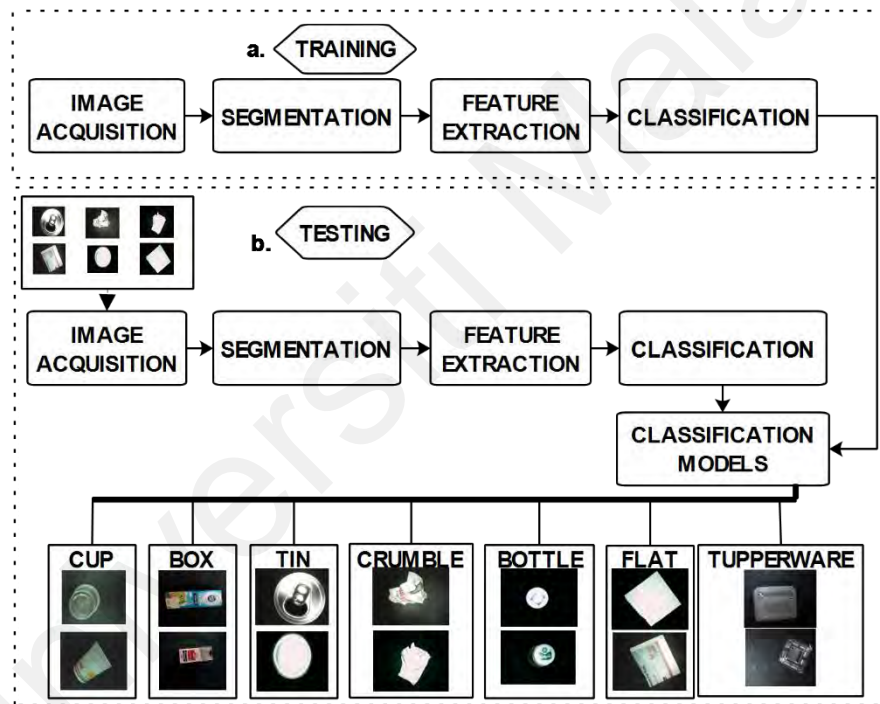


Figure 3.1: Overview of training and testing of the proposed system

The flowchart of the methodology for the research work is shown in figure below.

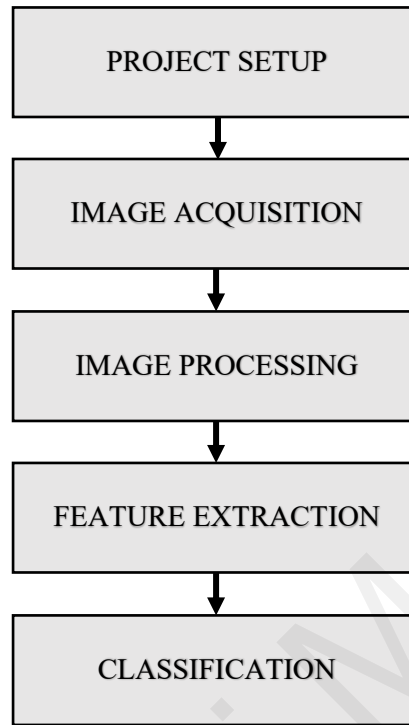


Figure 3.2: Methodology Flowchart

3.2 Project Setup

The prototype of the ASC system for garbage sorting is shown in Figure 3.2. The project is composed of vision system, various mechanical, electronics and electropneumatic parts and components. The bill of material for the whole project is shown in Appendix E.

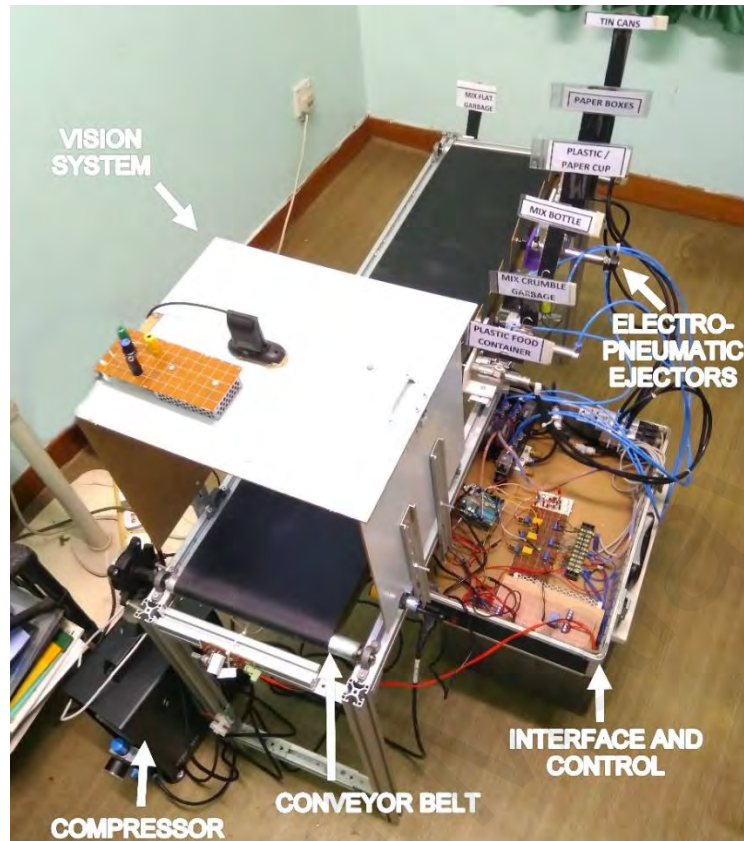


Figure 3.3: Automatic Sorting Conveyor (ASC) prototype

3.2.1 Mechanical Components

The conveyor mechanical assembly was composed of rigid industrial aluminum profile which support the structure of the conveyor. The carbon steel connection joints were used to do the connection between profile bars. Steel conveyor rollers were used for the conveyor belt and mounted on the profile bar with pillow block bearings. Appendix A shows the details of the all mechanical parts used in the project.

3.2.2 Electronics/Electrical Components

The project consists of various electronics and electrical components. Appendix B provides the details of the components and Appendix C shows the schematic diagram of the

control system with the outputs. The block diagram of the control interface is shown in Figure below.

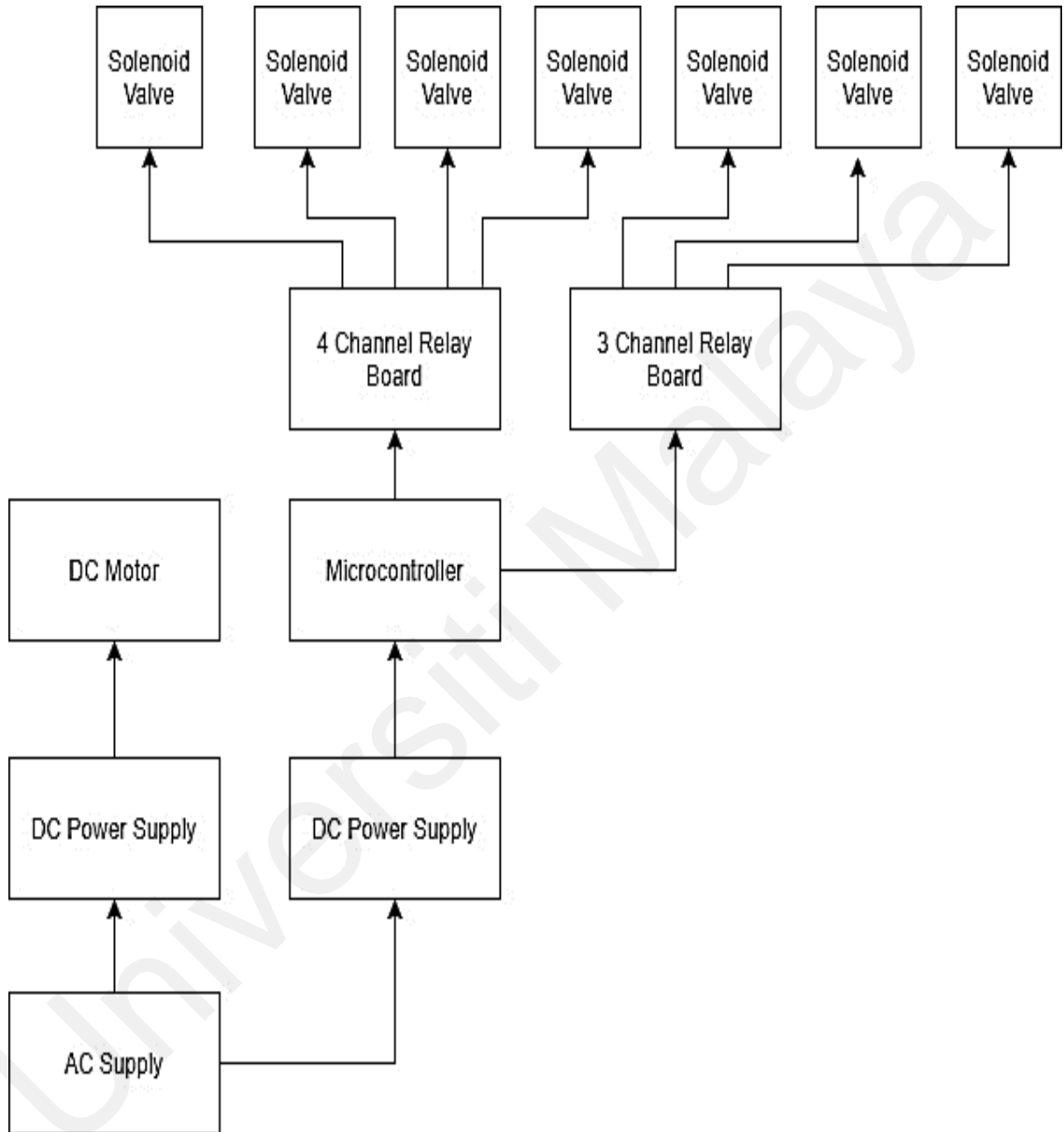


Figure 3.4: Control system block diagram of the ASC system

3.2.3 Electropneumatic Components

In this project we used 5/2 way monostable and bistable electrically actuated valves which activate and deactivate double acting cylinders to sort the garbage. The pneumatic and electro-pneumatic circuit diagrams are shown below and details of each component is given in Appendix D.

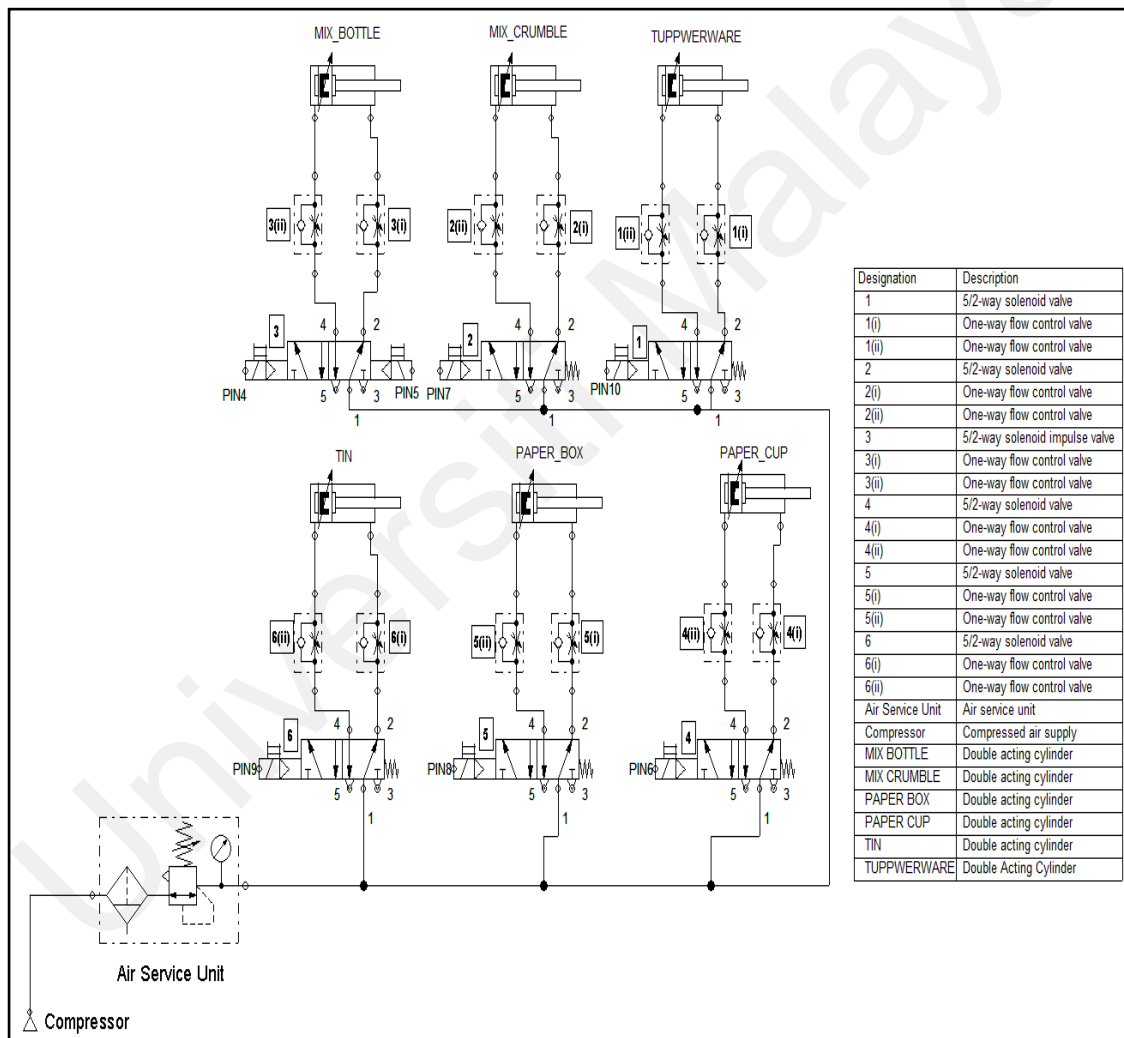


Figure 3.5 : Electro-Pneumatics Circuit Diagram

3.2.4 Conveyor Specifications

The specification of the conveyor system is provided in the table below:

| No | Item | Specification |
|----|----------------------------|----------------------|
| 1 | Length | 1.2 m |
| 2 | Width | 0.3 m |
| 3 | Speed | 20 RPM |
| 4 | Electro-Pneumatic Ejectors | 6 |
| 5 | Ejector Pressure | 5 bar |
| 5 | Image Acquisition Hardware | Logitech Webcam C310 |
| 6 | Control | Microcontroller |
| 7 | Image Inspection Area | 0.3m x 0.3m x 0.34m |

3.3 Image acquisition

After the conveyor setup the image acquisition of the dry waste garbage samples was performed. Figure 3.6 shows the block diagram and Fig 3.7 shows the actual picture of the ASC system prototype.

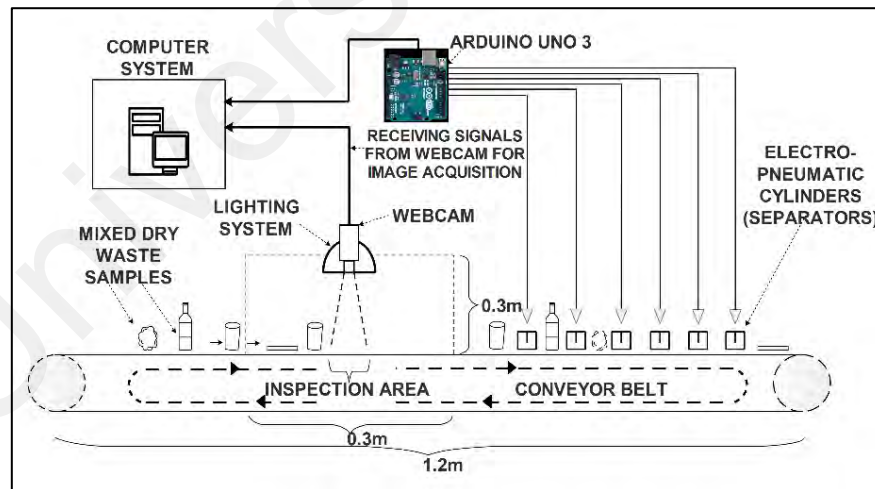


Figure 3.6: Block diagram: Automatic Sorting Conveyor (ASC) for garbage

Figure 3.7 also shows the components of the ASC system. The inspection zone as shown in Figure 3.8 is covered with acrylic sheet housing (0.3m x 0.3m x 0.34m) where the images of the dry waste garbage samples were taken on a 1.2m long conveyor running at speed of 1m/s from web camera (Logitech HD Webcam C310) for classification, attached at the center of the top acrylic sheet cover. The distance of the camera from the conveyor belt inspection area is 30 cm.

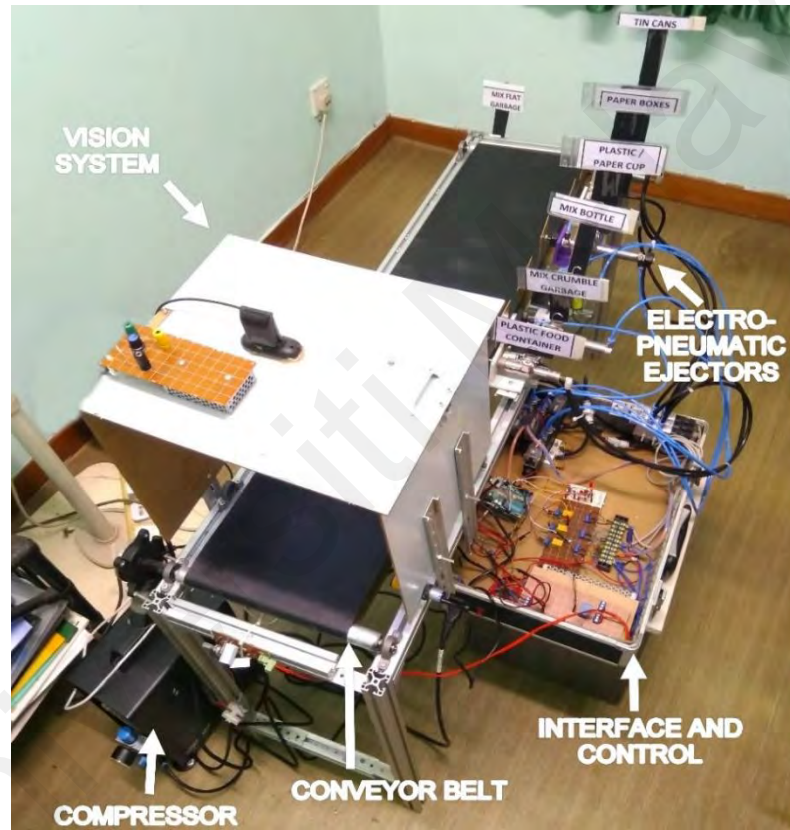


Figure 3.7: Actual system: Automatic Sorting Conveyor (ASC) for garbage



Figure 3.8: Inspection area of the ASC system

The properties setting for the camera such as brightness, contrast and saturation are adjusted based on their respective scales. For the illumination technique, array of light emitting diodes were used to provide homogenous lighting for the experiment to obtain a set of geometric properties i.e., size, shape, orientation and position of the dry waste samples. The whole classification and sorting process of the proposed system is shown in Figure 3.9.

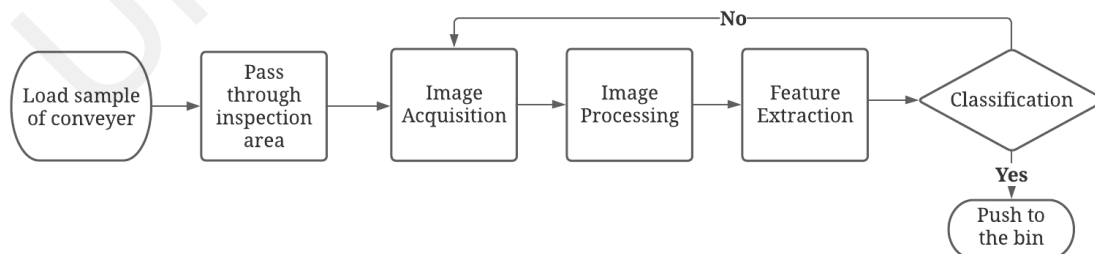


Figure 3.9: ASC system operational flowchart

In this experimental study, 320 sample images were taken for training and 320 samples for testing. All the samples were taken from rubbish bins from different public places such as homes, offices, shops and markets. The samples are of seven different types and number for each sample for training and testing is shown in Table 3.4. Figure 3.10 shows the subset of the images for each class, it can be seen that each image has different size, shape and orientation.

Table 3.1: Number of training and testing samples for each class

| No | Class for Dry Garbage Waste | Number of training samples | Number of testing samples |
|----|-----------------------------|----------------------------|---------------------------|
| 1 | Crumble (Paper/Plastic) | 50 | 50 |
| 2 | Flat (Paper/Plastic) | 50 | 50 |
| 3 | Tin Can | 50 | 50 |
| 4 | Bottle (Plastic/Glass) | 40 | 40 |
| 5 | Cup (Paper/Plastic) | 50 | 50 |
| 6 | Plastic Box | 40 | 40 |
| 7 | Paper Box | 40 | 40 |

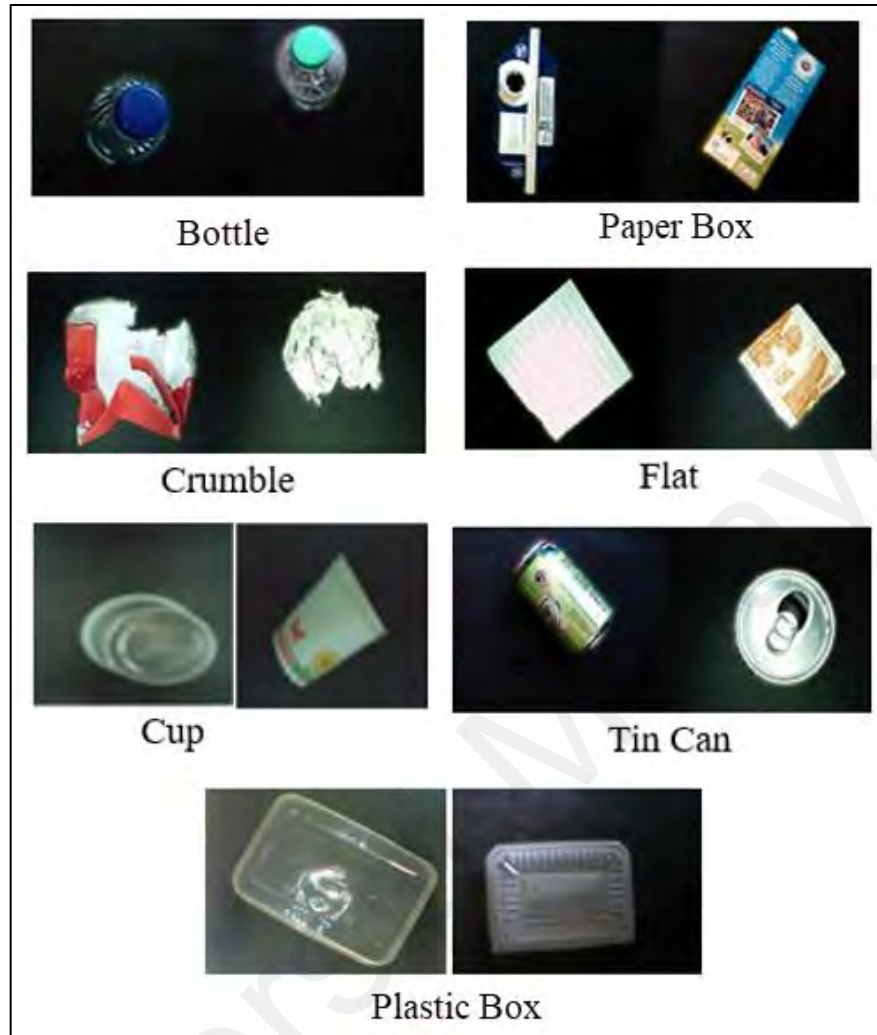


Figure 3.10: Sample images from training dataset

3.4 Image processing

The first operation for the feature extraction for classification is image processing. In order to extract good and important features from images, images need to be pre-processed (Rahman et al., 2011). Whichever method of segmentation is applied, it provides the building blocks of object base image analysis. (Hay & Castilla, 2008). Figure 3.11 shows the flow chart of the image processing for segmentation.

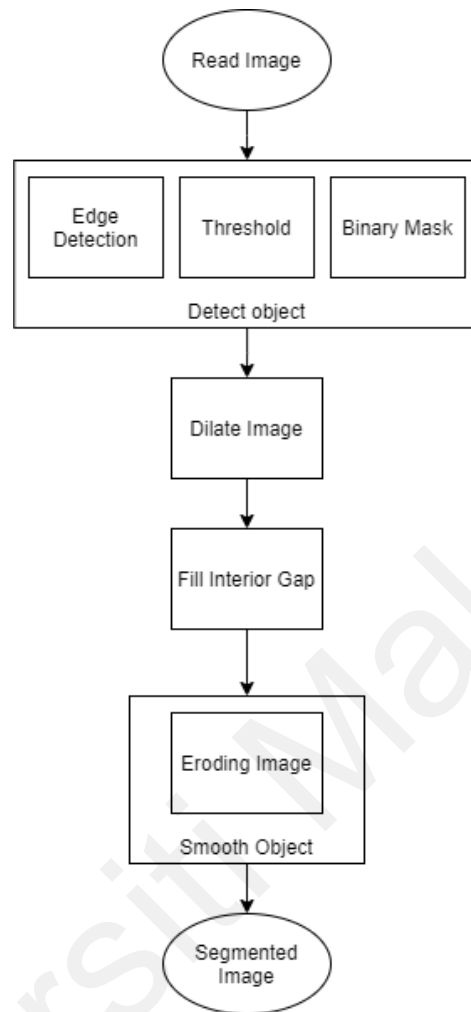


Figure 3.11: Image processing: Segmentation process flow chart

Matlab 2019b was used for the image processing, RGB image with size of 640x480 pixels was read by the software. We converted the RGB values of the image to the grayscale values because the grayscale images have 2-dimension and faster to process by the software. The grayscale of the images was obtained by calculating the weighted sum of R, G and B components.

$$grayscale = 0.30 * R + 0.59 * G + 0.11 * B \quad (3.1)$$

The object which was needed to be detected was entirely different in contrast from the background. We calculated gradient of the sample image and then applied the threshold. Sobel operator was used for edge detection. Sobel operator is one of the most commonly use edge detection techniques. It is inexpensive in terms of computation, as it involves convolving the image with horizontal and vertical filters with small, separable and integer values. It has advantage of proving smoothness and differentiation at same time. Figure 3.12 shows the comparison of output images from different edge detection techniques.

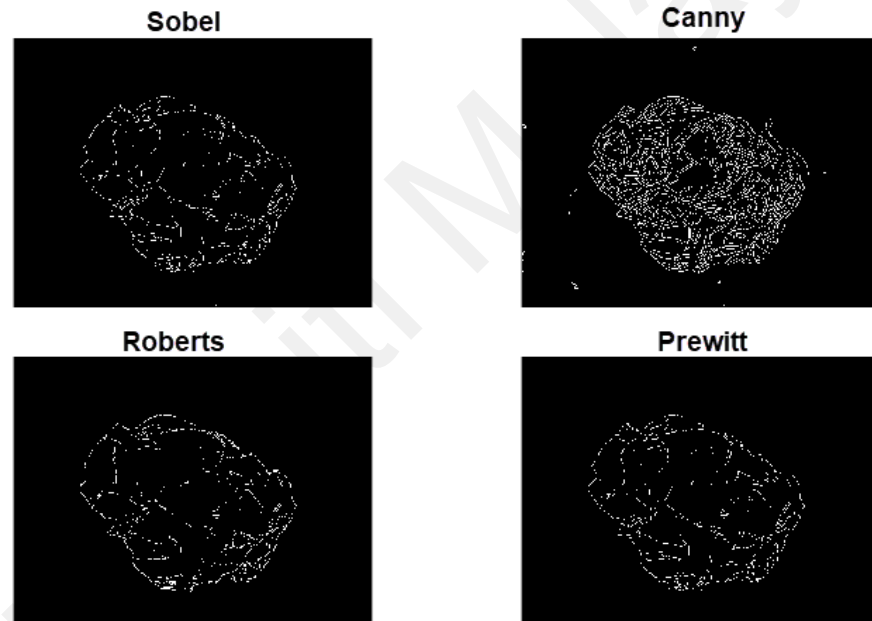


Figure 3.12: Comparison of edge detection techniques for sample images

The binary gradient mask was the output of the edge detection step. The next step in the image processing was dilation. Structuring element is an essential part of the morphological dilation. In this process disk-shaped structuring elements were used, with the radius of 4 and 4 number of structuring element lines to approximate the disk shape. Then filled the interior gaps and holes of the output binary image and did the erosion to smoothen the object. The final output

of the process was the segmentation filter; therefore, the area of the sample garbage image can be extracted from the background. Segmentation flow process for each type of class sample is shown in Figure 3.13.



Figure 3.13: Segmentation stages for bottle class sample

3.5 Feature Extraction

The proposed system returned up to 40 features; however, 17 best features were selected for classification. Table 3.5 shows the list of the features used for classification and sort the waste garbage samples. F1 and F2 are from white pixel plot and F3 – F17 are from grey scale of the segmented image samples. Description of each feature is discussed in following sections.

Figure 3.30(a) shows the binary image which is used for the segmentation filter for the sample images. A white pixel array C , was created from the segmentation filter of the sample images and was used to create a plot for each of sample image.

As shown in Table 3.5 quantile value (F1) was calculated from array C . The features like standard deviation, pixel intensity, GLCM, entropy and mean of the Gabor filter magnitudes were calculated from grey scale image of the segmented sample images.

Table 3.2: List of Features

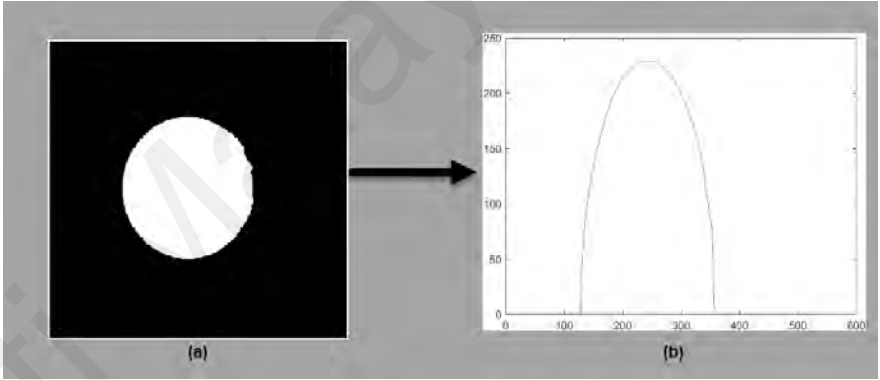
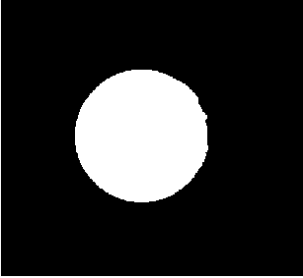

| Feature No | Feature Name | Feature Source | Reference Figures |
|------------|----------------|---|---|
| F1 | Quantile Value | Array C, created from the sum of white pixel in each row of the segmentation filter image. The size of the image 640x480 pixels. Array C for each sample image was 640 row matrix. The plot for a sample is shown in Figure 3.30 (b). |  <p>Figure 3.14 consists of two parts. Part (a) is a square image with a black background and a white circle in the center, labeled '(a)'. An arrow points from part (a) to part (b). Part (b) is a line graph showing a bell-shaped curve. The x-axis is labeled from 0 to 600 in increments of 100. The y-axis is labeled from 0 to 250 in increments of 50. The curve starts at approximately x=100, reaches a peak of about 230 at x=250, and ends at approximately x=400. It is labeled '(b)'.</p> <p>Figure 3.14: (a) Segmentation Filter (b) Graph of summation of white pixel for each column</p> |
| F2 | Entropy | Segmentation Filter Image |  <p>Figure 3.15 is a square image with a black background and a white circle in the center, identical to the one in Figure 3.14(a). It is labeled 'Figure 3.15: Segmentation Filter'.</p> <p>Figure 3.15: Segmentation Filter</p> |

Table 3.5: List of Features (Continued)

| Feature No | Feature Name | Feature Source | Reference Figures |
|------------|---|------------------------------|--|
| F3 | Standard Deviation | Greyscale of Segmented Image |  <p data-bbox="1325 1045 1671 1114">Figure 3.16: Greyscale of Segmented Image</p> |
| F4 | Grey Pixels Intensity (>180 and \leq 255) | | |
| F5 | Grey Pixels Intensity (>40 and \leq 110) | | |
| F6 | Contrast (Grey-Level Co-Occurrence Matrix) | | |
| F7 | Correlation (Grey-Level Co-Occurrence Matrix) | | |
| F8 | Energy (Grey-Level Co-Occurrence Matrix) | | |
| F9 | Homogeneity (Grey-Level Co-Occurrence Matrix) | | |
| F10 | Entropy | | |
| F11-F17 | Mean of Gabor Filter Magnitudes | | |

3.5.1 Quantile Value

Quantile determined how many values in a distribution are above or below a certain limit. It is also referred to dividing a probability distribution into areas of equal probability. F1 was calculated as the maximum value of quantile of array C . The equation shows the formulation of F1.

$$F1 = \max(\text{quantile}(C, p)) \quad (3.2)$$

Where p represents cumulative probability and C is the row array of the white pixels of image.

3.5.2 Entropy

Entropy is the statistical measure of randomness that can be used to characterize the texture of the input image (Gonzalez & Woods, 2008). Entropy function gives a value to represents level of complexity in a certain section of image. It is very important to have higher entropy in order to have precise segmented image post-processing method so that it can classify accordingly to its own type of groups. The entropy algorithm is shown in Equation 3.3.

$$= -\text{sum}(p.* \log_2(p)) \quad (3.3)$$

Where p represents the normalized histogram counts.

3.5.3 Standard deviation

It is the measure of the amount of variation or dispersion of a set of values. A low standard deviation indicates that the values tend to be close to the mean of the set, while a high standard deviation indicates that the values are spread out over a wider range. Standard deviation filter can be very advantages for radar images. Formally, interpretation of radar images quite

hard because of back scatter (return of the pulse sent by the radar). This is due to a lot of “noise”. Therefore, some pattern can be recognizable when using standard deviation filter.

For a random variable vector, A made up of N scalar observations, the standard deviation is defined as:

$$S = \sqrt{\frac{1}{N-1} \sum_{i=1}^N |C_i - \mu|^2} \quad (3.4)$$

Where C represents metric of the greyscale of the segmented image with N number of values greater than 0, and μ is the mean of C .

3.5.4 Ratio of grey level

Grey level is fundamental in study of image processing. The grey level or grey value indicates the brightness of a pixel. The maximum grey value depends on the depth of an image. For example, 8-bit-deep image contain levels up to 255, which they can take any value in the range. However, binary image can only take either value 0 or 255. Table 3.6 shows the summary of grey level.

The program has been setup to calculate ratio of low grey level (L) and ratio high of grey level (H) to the total grey pixels. Here, ratio of grey level (L) is denoting as $40 < x = 110$, and ratio of grey level (H) is denoted as $181 = x = 255$.

Table 3.3: Grey values level for color

| Grey level | Color |
|---------------|-------|
| 0 | Black |
| $0 < x < 255$ | Grey |
| 255 | White |

3.5.5 Grey level co-occurrence matrix

Another statistical technique that contemplates with spatial relationship of pixels is the grey level co-occurrence matrix (GLCM). GLCM works by calculating how often a pixel with the intensity value i occurs in a specific spatial relationship to a pixel with the value j . By default, the spatial relationship is defined as the pixel of interest and the pixel to its immediate right (horizontally adjacent). Each element (i,j) in the resultant is simply the sum of the number of times that the pixel with value i occurred in the specified spatial relationship to a pixel with value j in the input image.

The number of grey levels is very significant as it can be used to determine the size of GLCM. Therefore, parameters such as number of grey levels and the scaling intensity values need to be controlled. The grey level co-occurrence matrix can reveal certain properties about the spatial distribution of the grey levels in the texture image. For example, if most of the entries in the GLCM are concentrated along the diagonal, the texture is coarse with respect to the specified offset. In MATLAB R2019b software, GLCM have been programmed to derive several statistical measures such as contrast, correlation, energy and homogeneity.

For contrast, it calculates the variation of localization point in the grey level co-occurrence matrix, as shown in Equation 3.5. For correlation, it measures the occurrence probability of joint in specified pairs of pixels, as shown in Equation 3.6. For energy, also widely known as uniformity or the angular second moment, providing addition of squared pixels in the GLCM, as shown in Equation 3.7. Lastly, homogeneity is to test the proximity of element distribution in the GLCM to the GLCM diagonal, as shown in Equation 3.8.

$$\text{Contrast} = \sum_{i,j} |i - j|^2 p(i, j) \quad (3.5)$$

Where p represents the normalised histogram counts and (i, j) are position values of pixels.

$$\text{Correlation} = \sum_{i,j} \frac{(i-\mu_i)(j-\mu_j)p(i,j)}{\sigma_i \sigma_j} \quad (3.6)$$

Where (i, j) represents position values of pixels and μ is the mean of the pixel at the position (i, j) . σ is standard deviation of pixel at the position (i, j) .

$$\text{Energy} = \sum_{i,j} p(i, j)^2 \quad (3.7)$$

Where p represents the normalised histogram counts and (i, j) are position values of pixels.

$$\text{Homogeneity} = \sum_{i,j} \frac{p(i, j)}{1 + |i - j|} \quad (3.8)$$

Where p represents the normalised histogram counts and (i, j) are position values of pixels.

There are some previous studies which implemented grey level co-occurrence matrix in waste sorting management. (Wang & Kong, 2011) proposed a system for waste recognition based on GLCM and probabilistic neural network. The technique obtains waste image from conveyor belt by high-speed camera, implement image pre-processing, extracts the texture features GLCM and then train using neural network. It is notable that from extracting GLCM features provide a resource way for waste disposal.

(Hannan et al., 2016) extract GLCM features parameters such as displacement, quantization and the number of textural features for a solid waste bin level detection. Based on

the results obtained, it has great outcome and potential to be used for solid waste bin level classification as it provides a robust solution in terms of detection, monitoring and management.

3.6 Classification

The aim of supervised machine learning is to build a model that makes predictions based on evidence in the presence of uncertainty. A supervised learning algorithm takes a known set of input data and known responses to the data (output) and trains a model to generate reasonable predictions for the response of new data (Paluszek & Thomas, 2016). Classification models classify input into categories.

The classification models used in this study are explained in detail with their specification in following sections.

3.6.1 Support Vector Machine (SVM)

SVM is the powered version of linear discriminant. For two classes it is just the straight line which divides the features values into two groups, one for each group. If more than two features are involved this line becomes a plane or a hyperplane (Parker, 2010). SVM belong to a subcategory of machine learning algorithms known as kernel methods, in which the features are transformed using a kernel function. Kernel functions map data to a different, often higher dimensional space with the assumption that the classes will be easier to distinguish as a result of the transformation, theoretically simplifying a complex non-linear decision boundary to linear decision boundaries in the higher dimensional, mapped feature space. The data does not need to be directly transformed in this method, which would be computationally costly. This is commonly known as kernel trick (*Support Vector Machine (SVM)*).

The attributes for SVM types are following:

Table 3.4: SVM classifiers attributes

| Classifier Type | Prediction Speed | Memory Usage | Interpretability | Model Flexibility |
|------------------------|------------------------------------|-------------------------------------|-------------------------|--------------------------|
| Quadratic SVM | Binary: Fast Multiclass: Medium | Binary: Medium Multiclass: Large | Hard | Medium |
| Cubic SVM | Binary: Fast Multiclass: Medium | Binary: Medium Multiclass: Large | Hard | Medium |

| | | |
|-------------------|--------|------------|
| Prediction Speed: | Fast | 0.01second |
| | Medium | 1second |
| Memory Usage: | Medium | 4MB |
| | Large | 100MB |

In our proposed study we have used SVM model implemented in MATLAB using Classification Learner Application. There are six SVM classifiers type in Classification Learner Application. For this study we have used Cubic SVM and Quadratic SVM.

The Quadratic SVM and Cubic SVM results were more accurate and higher as compared to other SVM classifier types. The parameters set for each model in this study are given in Table 3.8.

Table 3.5: SVM classifier types and their parameters selected

| Type of SVM | Parameters | | | |
|--------------------|--------------------------|-----------------------------|--------------------------|-------------------------|
| | Kernel scale mode | Box constraint Level | Multiclass method | Standardize data |
| Quadratic | Automatic | 1 | One-vs-One | Yes |
| Cubic | Automatic | 1 | One-vs-One | Yes |

3.6.2 K-Nearest Neighbour:

Since it is simple and produces good results, the nearest neighbor approach is widely used in classifiers. But, if one neighbor produces good results, why not use several? The k-nearest neighbor method is based on this basic idea, in which the class is decided by a vote between the nearest k neighbors in feature space. There are two main ways to do this: compute all distances, arrange them into descending order, and read off the smallest k, or hold only the smallest k in a table and test/insert after each distance measurement (Parker, 2010).

The key advantages of this approach are its simplicity (e.g., no assumptions about the probability distributions of each class are required) and versatility (e.g., no assumptions about the probability distributions of each class are required) (e.g., it handles overlapping classes or classes with complex structure well). The key drawback is the computational cost of computing distances between the unknown sample and several (potentially all) stored points in the feature space using a brute force method (Marques, 2011).

Table 3.6: KNN classifier attributes

| Classifier Type | Prediction Speed | Memory Usage | Interpretability | Model Flexibility |
|------------------------|-------------------------|---------------------|-------------------------|--|
| Fine KNN | Medium | Medium | Hard | Finely detailed distinctions between classes. The number of neighbors is set to 1. |
| Medium KNN | Medium | Medium | Hard | Medium distinctions between classes. The number of neighbors is set to 10. |

Table 3.9: KNN classifier attributes (continued)

| Classifier Type | Prediction Speed | Memory Usage | Interpretability | Model Flexibility |
|------------------------|-------------------------|---------------------|-------------------------|--|
| Coarse KNN | Medium | Medium | Hard | Coarse distinctions between classes. The number of neighbors is set to 100. |
| Cosine KNN | Medium | Medium | Hard | Medium distinctions between classes, using a Cosine distance metric. The number of neighbors is set to 10. |
| Cubic KNN | Slow | Medium | Hard | Medium distinctions between classes, using a cubic distance metric. The number of neighbors is set to 10. |
| Weighted KNN | Medium | Medium | Hard | Medium distinctions between classes, using a distance weight. The number of neighbors is set to 10. |

In the KNN procedure, the labels of the k closest neighboring samples are used to mark each point in the input space (where distances are computed according to a given metric, often the Euclidean norm). The only parameter that requires tuning in k -NN is k , the value of the number of samples in the considered neighborhood: the choice of k is usually data-driven (often decided though cross-validation) (Susto et al., 2015). Larger values of k minimise the impact of noise on classification, but they blur the distinction between groups (Zhang & Zhou, 2007).

The parameters of the KNN classifier model are shown in Table 3.10 below. Cost matrix applied in this experiment are using the default setting of misclassification costs.

Table 3.7: KNN parameters selected

| Type of KNN | Parameters | | | |
|-------------|---------------------|-----------------|-----------------|------------------|
| | Number of Neighbors | Distance metric | Distance weight | Standardize data |
| Fine | 1 | Euclidean | Equal | True |

3.6.3 Ensemble

In complex situations with many classes and features, it is common to find that some classifiers perform better for some classes than others. It's also possible that certain classifiers perform better under some lighting conditions or in the presence of particular types of noise. In such cases, using more than one type of classifier and combining the results after classification might be optimal. These are referred to as ensemble classifiers. The trick to using an ensemble is to figure out how to combine the various findings from the different classifiers. And if the problem has been spread, they might be of very different types and use very different approaches, but they all share the same basic purpose (Parker, 2010).

Ensemble classification methods combine the responses of many weak classifiers to achieve better predictive efficiency than any of their constituent methods. This approach is well suited to industrial machine vision applications because of these characteristics (Shaukat et al., 2016). Matlab 2019b has following types of Ensemble classifier and the qualities of each type is shown in Table 3.11 below.

Table 3.8: Ensemble classifier types and their attributes

| Classifier Type | Prediction Speed | Memory Usage | Interpretability | Ensemble Method | Model Flexibility |
|---------------------------|-------------------------|---------------------|-------------------------|--|--------------------------|
| Boosted Trees | Fast | Low | Hard | AdaBoost, with Decision Tree learners | Medium to high |
| Bagged Trees | Medium | High | Hard | Random forest Bag, with Decision Tree learners | High |
| Subspace Discriminant | Medium | Low | Hard | Subspace, with Discriminant learners | Medium |
| Subspace KNN | Medium | Medium | Hard | Subspace, with Nearest Neighbor learners | Medium |
| RUSBoosted Trees | Fast | Low | Hard | RUSBoost, with Decision Tree learner | Medium |
| GentleBoost or LogitBoost | Fast | Low | Hard | GentleBoost or LogitBoost, with Decision Tree learners Choose Boosted Trees and change to GentleBoost method. | Medium |

In this study, we used Ensemble Boosted Trees classifier and the parameters used in the software are shown in Table 3.12 below.

Table 3.9: Ensemble boosted trees classifier parameters selected

| Type of Ensemble | Parameters | | | |
|-------------------------|---------------------------------|---------------------------|----------------------|---------------------------|
| | Maximum number of splits | Number of learners | Learning rate | Subspace dimension |
| Boosted Trees | 20 | 30 | 0.1 | 1 |

CHAPTER 4: RESULTS AND DISCUSSION

There were total of 640 samples for 7 dry waste garbage classes were used in this experiment. For training purpose 320 sample images were taken for training and 320 sample images for testing.

4.1 Training and testing dataset

In this study 320 sample images were taken for 7 different dry waste garbage classes. The features data was extracted from greyscale, segmented greyscale images and binarized image of the captured RGB images using the Matlab 2019b. The result produced a feature vector which had 17 values and result from all images was stored in the excel file for all 320 images. The excel file contained features data for all 320 sample images called dataset and each class data column has its' respective label to perform the accurate training.

The testing 320 sample images were put randomly in the folder for the purpose of the testing. The testing was also performed using Matlab 2019b. The testing sample images folder was not given any name and were identified one by one by the software. However, the accurate name for each sample was stored in excel file for the purpose to calculate the accurate percentage of the classification results after performing the testing. The training and testing number of images for each class is shown in following table.

Table 4.1: No of samples for each class in dataset

| Class Name | No of training samples | No of testing samples |
|-------------------------|------------------------|-----------------------|
| Crumble (Paper/Plastic) | 50 | 50 |
| Flat (Paper/Plastic) | 50 | 50 |
| Tin Can | 50 | 50 |

Table 4.1: No of samples for each class in dataset (Continued)

| Class Name | No of training samples | No of testing samples |
|------------------------|------------------------|-----------------------|
| Bottle (Plastic/Glass) | 40 | 40 |
| Cup (Paper/Plastic) | 50 | 50 |
| Plastic Box | 40 | 40 |
| Paper Box | 40 | 40 |

4.2 Features Selection

Feature selection process was accomplished in four stages.

4.2.1 First Stage of Features Selection

In this study at beginning of the process at first stage there were total of 40 features were extracted from the sample images of each class. These features were taken from greyscale of segmented images, binarized segmented images and white pixel location array of the binarize images. The list of the 40 features is shown in Table 4.2.

Table 4.2: List of 40 features for classification

| Feature No | Name | Source Image/Graphs | Formula |
|------------|--------------------------------|------------------------------|--|
| F1 | Round Measure of Sample Images | Greyscale of Segmented Image | $= 4\pi A/P^2 \quad (4.1)$ where, A is the area P is the perimeter |

Table 4.2: List of 40 features for classification (Continued)

| Feature No | Name | Source Image/Graphs | Formula |
|------------|---------------------|---|--|
| F2 | Mid-Point Symmetry | Graph of array C, obtained from Segmentation Filter binarized image | $= \frac{o \sum_{y=1}^n d(y)=1}{\sum_{z=1}^n C1(z)} * 100$ (4.2) where; o is the total number of elements and y is the corresponding number of elements of array d, z is the corresponding elements of C1 array. |
| F3 | Skewness | Graph of array C, obtained from Segmentation Filter binarized image | $\frac{E(C-\mu)^3}{\sigma^3}$ (4.3) |
| F4 | Mode | | $= ((n + 1)/2)$ (4.4) |
| F5 | Kurtosis | | $= \frac{\sum(C-\mu)^4}{\sigma^4}$ (4.5) |
| F6 | Mean | | $= \frac{1}{N} \sum_{i=1}^N C_i$ (4.6) |
| F7 | Standard Deviation | | $S = \sqrt{\frac{1}{N-1} \sum_{i=1}^N C_i - \mu ^2}$ (4.7) |
| F8 | Zero-Scores | | $n \left[\left \frac{x-\mu}{\sigma} \right > 2 \right]$ (4.8) Where n is the total numbers of absolute value array, μ is the mean and σ is the standard deviation of the C. |
| F9 | Quantile | | $= \max(\text{quantile}(C, p))$ (4.9) where; $p = 25$ |
| F10 | Derivative Variance | | $\frac{1}{N-1} \sum_{i=1}^N C_i - \mu ^2$ (4.10) |
| F11 | Standard Deviation | Greyscale of Segmented Image | $S = \sqrt{\frac{1}{N-1} \sum_{i=1}^N A_i - \mu ^2}$ (4.11) |

Table 4.2: List of 40 features for classification (Continued)

| Feature No | Name | Source Image/Graphs | Formula |
|------------|--|---|--|
| F12 | Entropy | Greyscale of Segmented Image | $= -sum(p.* log2(p))$ (4.12) |
| F13 | Ratio of Greyscale Level Range (>40 and <111) to whole Greyscale Image | | $= A(\sum_{n=41}^{110} A(n-1) \& A(n))$ (4.13) |
| F14 | Ratio of Greyscale Level Range (>110 and <181) to whole Greyscale Image | | $= A(\sum_{n=41}^{110} A(n-1) \& A(n))$ (4.14) |
| F15 | Ratio of Greyscale Level Range (>180 and <=255) to whole Greyscale Image | | $= A(\sum_{n=181}^{255} A(n-1) \& A(n))$ (4.15) |
| F16 | Grey Level Co-Occurrence Matrix (Contrast) | | $\sum_{i,j} i-j ^2 p(i,j)$ (4.16) |
| F17 | Grey Level Co-Occurrence Matrix (Correlation) | $\sum_{i,j} \frac{(i-\mu_i)(j-\mu_j)p(i,j)}{\sigma_i \sigma_j}$ (4.17) | |
| F18 | Grey Level Co-Occurrence Matrix (Energy) | $\sum_{i,j} p(i,j)^2$ (4.18) | |
| F19 | Grey Level Co-Occurrence Matrix (Homogeneity) | $\sum_{i,j} \frac{p(i,j)}{1+ i-j }$ (4.19) | |
| F20 | Entropy | Segmentation Filter binarized image | $= -sum(p.* log2(p))$ (4.20) |

Table 4.2: List of 40 features for classification (Continued)

| Feature No | Name | Source Image/Graphs | Formula |
|------------|--------------------------------|--|--|
| F21 | Mean of Gabor Filers Magnitude | Gabor filters which were created from segmented grey image, with 4 different frequencies f , and 6 different wavelengths λ . | $f = [0, 90, 135, 45]$ (4.21) $\lambda = [2.8, 5.65, 11.314, 22.63, 45.25, 90.51]$ (4.22) |
| F22 | | | |
| F23 | | | |
| F24 | | | |
| F25 | | | |
| F26 | | | |
| F27 | | | |
| F28 | | | |
| F29 | | | |
| F30 | | | |
| F31 | | | |
| F32 | | | |
| F33 | | | |
| F34 | | | |
| F35 | | | |
| F36 | | | |
| F37 | | | |
| F38 | | | |
| F39 | | | |
| F40 | | | |

The 40 features did not provide the good result for the classifier training, which was less than 80% for each type of classifier. Several tests were conducted and number of redundant features, the features which contribute less and reduced the percentage rate of classification were removed from the list.

4.2.2 Second Stage of Feature Selection

On second stage, 20 features were selected from the 40 features and the classification accuracy was checked for each classifier. The list of 20 features is shown in Table 4.3. The sources and formulae for each feature are discussed in Table 4.2. After many experiments on different features combinations, it was observed that the features F1-F5, F7, F8, F10, F14, F30-F35, F37-F40 were insignificant and did not contribute much in classification process. After removing these features, the classifier training results were higher as compared to results from 40 features.

Table 4.3: List of 20 features for classification

| No | Feature No | Name |
|----|------------|--|
| 1 | F4 | Mode |
| 2 | F9 | Quantile |
| 3 | F11 | Standard Deviation |
| 4 | F12 | Entropy |
| 5 | F13 | Ratio of Greyscale Level Range (>40 and <111) to whole Greyscale Image |
| 6 | F15 | Ratio of Greyscale Level Range (>180 and <=255) to whole Greyscale Image |
| 7 | F16 | Grey Level Co-Occurrence Matrix (Contrast) |
| 8 | F17 | Grey Level Co-Occurrence Matrix (Correlation) |
| 9 | F18 | Grey Level Co-Occurrence Matrix (Energy) |
| 10 | F19 | Grey Level Co-Occurrence Matrix (Homogeneity) |
| 11 | F20 | Entropy |
| 12 | F21 | Mean of Gabor Filters Magnitude |
| 13 | F22 | |
| 14 | F23 | |
| 15 | F24 | |
| 16 | F26 | |
| 17 | F27 | |
| 18 | F28 | |
| 19 | F29 | |
| 20 | F36 | |

4.2.3 Third Stage of Feature Selection

The 20 features improved the classifier training accuracy; however, it did not improve significantly. Furthermore, in third stage three more features were removed to check the classifier accuracy. F4, F29 and F36 were removed from the list for the classifier training purpose. The training results showed increase in the training rate and classifiers accuracy reached up to 90.69%. The list of 17 features with the source figures, formulae and description are shown in Table 3.4 in methodology section.

4.2.4 Fourth Stage of Feature Selection

To testify the hypothesis and confirm the best feature for classifier training. We removed two more features to verify if more accuracy can be achieved. F4 and F9 were removed from the dataset of features. However, instead of increase in the accuracy of the classifiers, the

percentage accuracies of the classifiers were decreased. It was concluded that 15 features cannot provide more accuracy than 17 features and the chosen 17 features are the best features for the classifiers training. Which also conclude that the F4 and F9 are very significant features for the classification process. The summary of the features used for each stage is given in Table 4.4 below.

Table 4.4: Summary of features chosen for each stage for classifier training

| Features No | Feature Name | Features | | | |
|-------------|---|-------------|--------------|-------------|--------------|
| | | Frist Stage | Second Stage | Third Stage | Fourth Stage |
| | | 40 | 20 | 17 | 15 |
| F1 | Round Measure of Sample Images. | / | | | |
| F2 | Mid-Point Symmetry | / | | | |
| F3 | Skewness | / | | | |
| F4 | Mode | / | / | | |
| F5 | Kurtosis | / | | | |
| F6 | Mean | / | | | |
| F7 | Standard Deviation | / | | | |
| F8 | Zero-Scores | / | | | |
| F9 | Quantile | / | / | / | |
| F10 | Derivative Variance | / | | | |
| F11 | Standard Deviation | / | / | / | |
| F12 | Entropy | / | / | / | / |
| F13 | Grayscale Level Ratio Range (>40 and <111) | / | / | / | / |
| F14 | Grayscale Level Ratio Range (>110 and <181) | / | | | |
| F15 | Grayscale Level Ratio Range (>180 and <=255) | / | / | / | / |
| F16 | Grey Level Co-Occurrence Matrix (Contrast) | / | / | / | / |
| F17 | Grey Level Co-Occurrence Matrix (Correlation) | / | / | / | / |
| F18 | Grey Level Co-Occurrence Matrix (Energy) | / | / | / | / |
| F19 | Grey Level Co-Occurrence Matrix (Homogeneity) | / | / | / | / |
| F20 | Entropy | / | / | / | / |

Table 4.4: Summary of features chosen for each stage for classifier training (Continued)

| Features No | Feature Name | Features | | | |
|-------------|---------------------------------|----------|----|----|----|
| | | 40 | 20 | 17 | 15 |
| F21 | Mean of Gabor Filters Magnitude | / | / | / | / |
| F22 | | / | / | / | / |
| F23 | | / | / | / | / |
| F24 | | / | / | / | / |
| F25 | | / | | | |
| F26 | | / | / | / | / |
| F27 | | / | / | / | / |
| F28 | | / | / | / | / |
| F29 | | / | / | | |
| F30 | | / | | | |
| F31 | | / | | | |
| F32 | | / | | | |
| F33 | | / | | | |
| F34 | | / | | | |
| F35 | | / | | | |
| F36 | | / | / | | |
| F37 | | / | | | |
| F38 | | / | | | |
| F39 | | / | | | |
| F40 | | / | | | |

4.3 Classification

There are total of 320 images used for classification for the training phase. Matlab 2019b classification learner app was used to perform the classification of the training set of images. The classification was repeated 10 times to take the average result of the classification. The cross validation was set to 5-fold for the training of the classifiers.

4.3.1 Classifier Training

Several tests were conducted to select the classifiers with the highest classification rate. The results for each run for 40, 20, 17 and 15 features are explained in following sections.

4.3.1.1 Classifier Training Results for 40 Features

The training was done ten times to take the average of the results for each classifier.

The results for each run are shown in Figure 4.1.

| Classification Accuracy (%) for 40 Features | | | | | | | | | | | |
|---|---------|---------|---------|---------|---------|---------|---------|---------|---------|----------|-------|
| | Trial 1 | Trial 2 | Trial 3 | Trial 4 | Trial 5 | Trial 6 | Trial 7 | Trial 8 | Trial 9 | Trial 10 | Avg |
| Q. Discriminant | Failed | Failed | Failed | Failed | Failed | Failed | Failed | Failed | Failed | Failed | ##### |
| Q. SVM | 79 | 78.7 | 79.6 | 79 | 77.8 | 78.7 | 78.1 | 80.2 | 79.6 | 79 | 78.97 |
| C. SVM | 80.2 | 79.3 | 79.9 | 79.3 | 79 | 77.8 | 78.7 | 80.2 | 80.6 | 80.9 | 79.59 |
| Fine. KNN | 69.4 | 73.8 | 73.8 | 74.1 | 75.3 | 71.9 | 74.4 | 74.1 | 71.9 | 74.4 | 73.31 |
| E. Boosted Trees | 77.2 | 75.6 | 74.4 | 79.3 | 78.1 | 78.7 | 81.5 | 78.7 | 78.1 | 79.9 | 78.15 |
| E. Bagged Trees | 79.6 | 78.1 | 80.2 | 78.1 | 78.4 | 81.2 | 76.9 | 79.6 | 78.7 | 79.3 | 79.01 |

Figure 4.1: Classifiers training results for 40 Features

From the Figure 4.1, it can be seen that each classifier result for training was not significant high. Especially Q. Discriminant classifier which failed for the classification process. For each type of classifier during different runs they provided some better result. For example, C.SVM, Q.SVM, E. Boosted Trees and E. Bagged Trees classifiers showed more than 80% result but during different runs.

During run 6 only E. Bagged Trees classifier showed training result up to 81.2% but at same time the other classifiers showed less than 80%. During run 7 only E. Boosted Trees classifier showed training result of 81.5%. However other classifiers showed results less than 80%. During run 8 Q. SVM and C. SVM both showed result of 80.2% and in run 10 only C. SVM showed result of 80.9%.

Then we took the average for each classifier training result and as shown in Figure 4.1 all classifiers overall result for training was less than 80%. C.SVM showed the highest result of 79.59% and Fine. KNN showed the least result of 73.31%.

4.3.1.2 Classifiers Training Results for 20 Features

Classifiers training for 20 features was also executed ten times to take the average result for each classifier. The result for each execution is shown in Figure 4.2.

| | Classification Accuracy (%) for 20 Features | | | | | | | | | | |
|------------------|---|---------|---------|---------|---------|---------|---------|---------|---------|----------|-------|
| | Trial 1 | Trial 2 | Trial 3 | Trial 4 | Trial 5 | Trial 6 | Trial 7 | Trial 8 | Trial 9 | Trial 10 | Avg |
| Q. Discriminant | 78.10 | 78.4 | 79.9 | 78.4 | 78.7 | 78.7 | 77.5 | 80.6 | 79 | 76.5 | 78.58 |
| Q. SVM | 79.6 | 83.6 | 82.1 | 80.6 | 82.4 | 81.2 | 82.1 | 82.1 | 82.7 | 77.8 | 81.42 |
| C. SVM | 81.2 | 80.6 | 81.2 | 82.4 | 80.6 | 83.3 | 80.2 | 79.3 | 83 | 80.9 | 81.27 |
| Fine. KNN | 75.9 | 76.2 | 77.2 | 77.2 | 74.7 | 77.2 | 75.3 | 76.9 | 77.8 | 74.1 | 76.25 |
| E. Boosted Trees | 74.4 | 78.7 | 78.1 | 78.7 | 78.4 | 78.4 | 75.9 | 76.5 | 79.9 | 76.2 | 77.52 |
| E. Bagged Trees | 78.1 | 79 | 79.6 | 79.6 | 79.3 | 79 | 78.4 | 81.2 | 80.2 | 76.9 | 79.13 |

Figure 4.2: Classifiers training results for 20 Features

From the Figure 4.2 it can be seen that each classifier result for training improve as compared to results of 40 features. For each type of classifier during different runs they provided some better result. For example, Q.SVM and C.SVM provided result more than 83.6% and 83.3% during run 2 and run 6 respectively.

During run 8 Q. Discriminant showed result of 80.6% and during run 9 E. Bagged showed results of 80.2%. Fine. KNN and E. Boosted Trees classifiers showed result less than 80% in all executions.

Then we took the average for each classifier training result and as shown in Figure 4.1. Q. SVM and C. SVM classifiers training accuracy percentage was much higher for 20 features

as compared to 40 features. Q.SVM classifier provided training accuracy rate of 81.42% and C.SVM classifier provided training accuracy rate of 81.27% for all classes.

4.3.1.3 Classifiers Training Result for 17 Features

To observe whether training accuracy rate can be higher, we removed three more features. The features which were contributing less in the classification. The result of the classifier training is shown in Figure 4.3.

| Classification Accuracy (%) for 17 Features | | | | | | | | | | | |
|---|---------|---------|---------|---------|---------|---------|---------|---------|---------|----------|-------|
| | Trial 1 | Trial 2 | Trial 3 | Trial 4 | Trial 5 | Trial 6 | Trial 7 | Trial 8 | Trial 9 | Trial 10 | Avg |
| Q. Discriminant | 85.40 | 85.10 | 83.60 | 84.80 | 85.10 | 86.50 | 84.00 | 85.30 | 84.80 | 85.60 | 85.02 |
| Q. SVM | 90.50 | 90.20 | 90.50 | 91.10 | 91.10 | 89.40 | 91.00 | 91.00 | 91.10 | 91.00 | 90.69 |
| C. SVM | 89.80 | 88.80 | 90.20 | 88.20 | 86.80 | 88.50 | 87.00 | 90.10 | 88.20 | 90.10 | 88.77 |
| Fine. KNN | 83.00 | 84.20 | 84.20 | 84.50 | 83.90 | 83.00 | 84.00 | 84.00 | 84.50 | 83.90 | 83.92 |
| E. Boosted Trees | 85.90 | 86.80 | 87.40 | 85.90 | 85.60 | 86.80 | 87.00 | 86.80 | 85.90 | 86.80 | 86.49 |
| E. Bagged Trees | 81.60 | 81.30 | 80.50 | 81.30 | 81.90 | 80.70 | 81.00 | 81.30 | 81.30 | 81.20 | 81.21 |

Figure 4.3: Classifiers training results for 17 Features

Figure 4.3 shows the result of classifiers training using 17 features. All classifier models showed high results for 17 features dataset.

Q. SVM and C. SVM classification models showed results above 90% for the training. Q. Discriminant showed result of 86.50% in run 6 whereas in other runs its result was also very good more than 84% for all runs. Fine. KNN showed result of 84.5% in run 3 and run 9 as well. E. Boosted Trees classifier showed result of 87.4% in run 3. Whereas E. Bagged Trees showed the least result of 81.90% in run 5 as compared to other classifiers.

The average result for all classifiers for all runs is also shown in Figure 4.3. Among all classification models, Q. SVM showed the highest result of 90.69% and E. Bagged Trees showed the least result of 81.21%.

4.3.1.4 Classifiers Training Result for 15 Features

| | Classification Accuracy (%) for 15 Features | | | | | | | | | | |
|------------------|---|---------|---------|---------|---------|---------|---------|---------|---------|----------|-------|
| | Trial 1 | Trial 2 | Trial 3 | Trial 4 | Trial 5 | Trial 6 | Trial 7 | Trial 8 | Trial 9 | Trial 10 | Avg |
| Q. Discriminant | 78.7 | 76.5 | 77.8 | 79 | 76.5 | 76.5 | 79.3 | 77.9 | 79 | 76.5 | 77.77 |
| Q. SVM | 81.5 | 80.2 | 83 | 82.7 | 81.5 | 80.9 | 81.8 | 81.5 | 82.5 | 82.7 | 81.83 |
| C. SVM | 82.1 | 79.9 | 82.4 | 80.9 | 83 | 82.4 | 80.2 | 82.2 | 80.8 | 83 | 81.69 |
| Fine. KNN | 78.4 | 76.9 | 75 | 77.2 | 79.6 | 78.1 | 77.2 | 78.2 | 77.2 | 78.2 | 77.60 |
| E. Boosted Trees | 77.5 | 76.5 | 75 | 77.2 | 79.3 | 76.9 | 81.2 | 77.4 | 77.2 | 77.9 | 77.61 |
| E. Bagged Trees | 78.1 | 77.8 | 76.9 | 79 | 77.2 | 77.2 | 76.2 | 78.1 | 76.9 | 78.1 | 77.55 |

Figure 4.4: Classifiers training results for 15 Features

Furthermore, two more features were removed from the dataset to check whether classifiers training accuracy can reach more higher value. As shown in Figure 4.4 the classifier results decreased instead. The highest accuracy was achieved by Q. SVM classifier of 82.7%. Other than Q. SVM and C. SVM, all classifiers showed average result less than 80%.

4.3.2 Classifier Selection

It was concluded that the 17 features dataset is the most fitting for the classification of dry waste sample classes. The Table 4.5 and Figure 4.5 below shows the summary of classification models result for 40, 20, 17 and 15 features dataset. The Q. SVM classification model from all classifiers were chosen, as it provided the highest classification accuracy rate of 90.69%. The Q. SVM was then used to perform the testing on the 320 samples for all classes.

Table 4.5: Training accuracy for each classifier for 40, 20, 17 and 15 features

| | No of Features | | | |
|-------------------------|------------------------------------|-------|--------------|-------|
| | 40 | 20 | 17 | 15 |
| Classifier | Classification Accuracy (%) | | | |
| Q. Discriminant | Failed | 78.58 | 85.02 | 77.77 |
| Q. SVM | 78.97 | 81.42 | 90.69 | 81.83 |
| C. SVM | 79.59 | 81.27 | 88.77 | 81.69 |
| Fine. KNN | 73.31 | 76.25 | 83.92 | 77.6 |
| E. Boosted Trees | 78.15 | 77.52 | 86.49 | 77.61 |
| E. Bagged Trees | 79.01 | 79.13 | 81.21 | 77.55 |

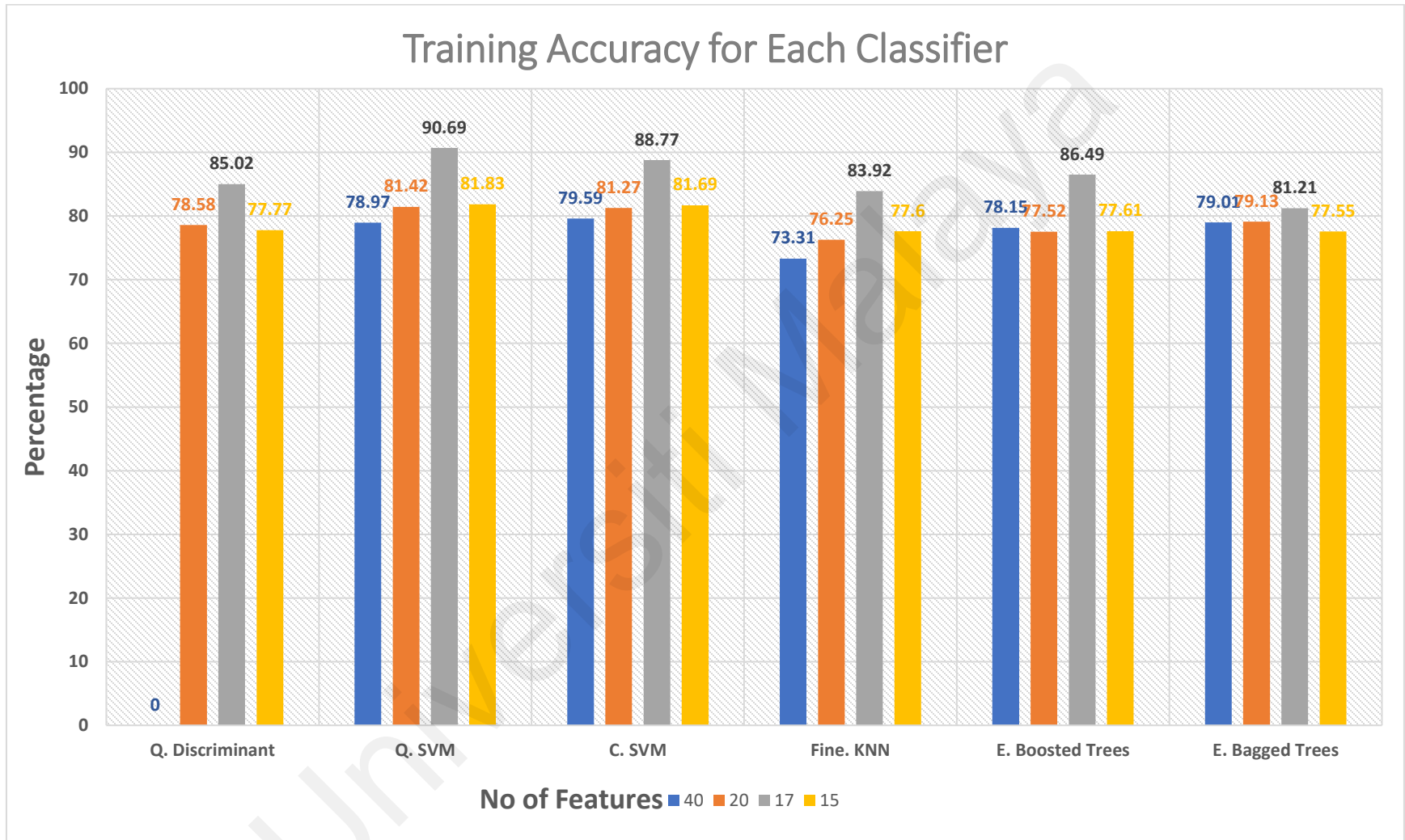


Figure 4.5: Training accuracy (%) of classifiers

4.3.3 Classifier Performance

Q. SVM classifier model obtained from the 17 features model training was used to perform the testing on 320 images. The test process was done five times on all testing database of images. Table 4.6 provided the testing results for the Q. SVM classifier for all classes. Each test run provides very promising accuracy for all classes. Crumble (Paper/Plastic) and Flat (Paper/Plastic) showed accuracy of 100%. The least classification accuracy was 76% of Bottle (Plastic/Glass) class. However, during run 3 it showed the accuracy of 78%. Tin Can, and Cup samples showed accuracy of above 90% for all runs. Except run 4 provided the Cup sample accuracy of 89%.

Table 4.6: Q. SVM Classifier Testing Accuracy

| Class | 17 Features | | | | | Average |
|--------------------------------|-------------|------|------|------|------|--------------|
| | Run1 | Run2 | Run3 | Run4 | Run5 | |
| Crumble (Paper/Plastic) | 100% | 100% | 100% | 100% | 100% | 100% |
| Flat (Paper/Plastic) | 100% | 100% | 100% | 100% | 100% | 100% |
| Tin Can | 95% | 92% | 94% | 94% | 95% | 94% |
| Bottle (Plastic/Glass) | 75% | 76% | 78% | 78% | 75% | 76% |
| Cup (Paper/Plastic) | 90% | 92% | 90% | 89% | 90% | 90% |
| Plastic Box | 85% | 84% | 86% | 85% | 84% | 85% |
| Paper Box | 82% | 84% | 83% | 85% | 84% | 84% |
| Overall Accuracy | | | | | | 89.9% |

The confusion matrix for the test run 3 is shown in Table 4.7 below. The 6% of Tin Can samples were misclassified as Crumble (Paper/Plastic). The Bottle samples were misclassified as Cup and Plastic Box with highest misclassification of 14% and 8% respectively, whereas Cup samples were misclassified as 5% Flat and 5% Tin samples. The Box samples were misclassified as 10% Flat and 7% Bottle samples respectively.

Table 4.7: Confusion matrix of Q.SVM model testing run 3

| Class | Crumble (Paper/Plastic) | Flat (Paper/Plastic) | Tin Can | Bottle (Plastic/Glass) | Cup (Paper/Plastic) | Plastic Box | Paper Box |
|--------------------------------|-------------------------|----------------------|------------|------------------------|---------------------|-------------|------------|
| Crumble (Paper/Plastic) | 100% | | | | | | |
| Flat (Paper/Plastic) | | 100% | | | | | |
| Tin Can | 6% | | 94% | | | | |
| Bottle (Plastic/Glass) | | | | 78% | 14% | 8% | |
| Cup (Paper/Plastic) | | 5% | 5% | | 90% | | |
| Plastic Box | | 4% | | | | 86% | 10% |
| Paper Box | | 10% | | 7% | | | 83% |

The Q. SVM classifier model acquired from 40, 20 and 17 features were also used to test the class testing database images. The summary of the Q. SVM classification result for 40, 20, 17 and 15 features are shown in Table 4.8 below.

Table 4.8: Q. SVM result summary for 40, 20, 17 and 15 features for all classes

| Class | No of Features | | | |
|--------------------------------|----------------|-------------|------|-----|
| | 15 | 17 | 20 | 40 |
| Crumble (Paper/Plastic) | 83% | 100% | 100% | 85% |
| Flat (Paper/Plastic) | 74% | 100% | 89% | 75% |
| Tin Can | 70% | 94% | 95% | 66% |
| Bottle (Plastic/Glass) | 71% | 76% | 59% | 71% |
| Cup (Paper/Plastic) | 72% | 90% | 71% | 69% |
| Plastic Box | 82% | 85% | 79% | 80% |
| Paper Box | 86% | 84% | 70% | 85% |

Table 4.9 shows for the Q. SVM classifier the 17 features dataset result provided the highest result for all classes except Box. The Box samples were 86% classified using 15 features. But 15 features dataset showed very poor classification accuracy for Flat, Tin Can, Bottle and Cup samples.

4.4 Classification Algorithm Application

The proposed classification algorithm was used for the sorting the garbage on the conveyor. The conveyor as shown in Figure 3.3 was used for that purpose. The testing sample garbage was put on conveyor and algorithm was run on Matlab image processing software. The image processing software performed the classification and provide the signal to the electro-pneumatic separator through the microcontroller. For each class there was one separator to push the garbage sample off the conveyor.

4.5 Discussion

The 640 images of dry waste were divided into two datasets. One dataset of 320 images were used for training of the classification model and remaining 320 images were used for the testing of the classification model. The 40 number of features were obtained from the training dataset of images. And were used for testing the classification model. Q. Discriminant, Q. SVM, C. SVM, Fine. KNN, E. Boosted Trees, E. Bagged Trees classifier were chosen for training the dataset. The classification results from the 40 features were less than 80%, for all classification models as shown in Table 4.5. Therefore, several tests conducted to take out the feature who contributed less in training the classification model. Then 20 features were selected for the training, the training accuracy result increase for all classification models except E. Boosted Trees. To increase the classification training accuracy three more features mode, two gabor filter magnitude features were removed from the features dataset. The result

for the classifier models training were remarkable. As shown in Table 4.5 all the classification models gave result more than 80%. The Q.SVM showed the highest of all the other classification models of 90.69%. Then Q.SVM was used on the testing images database for the classification. The testing results as shown in Figure 4.6 for the Q.SVM for all classes were very good. Crumble and Flat samples classification result was 100%. The Tin Can shows second highest of 94%. Then later was class Cup with 90% classification accuracy. The Plastic Box class and Paper Box class showed classification accuracy of 85% and 84% respectively. The least classification accuracy was of 76% of Bottle class. The overall accuracy of Q.SVM for all samples was 89.9%. The classification model was used to separate the garbage samples from the conveyor.

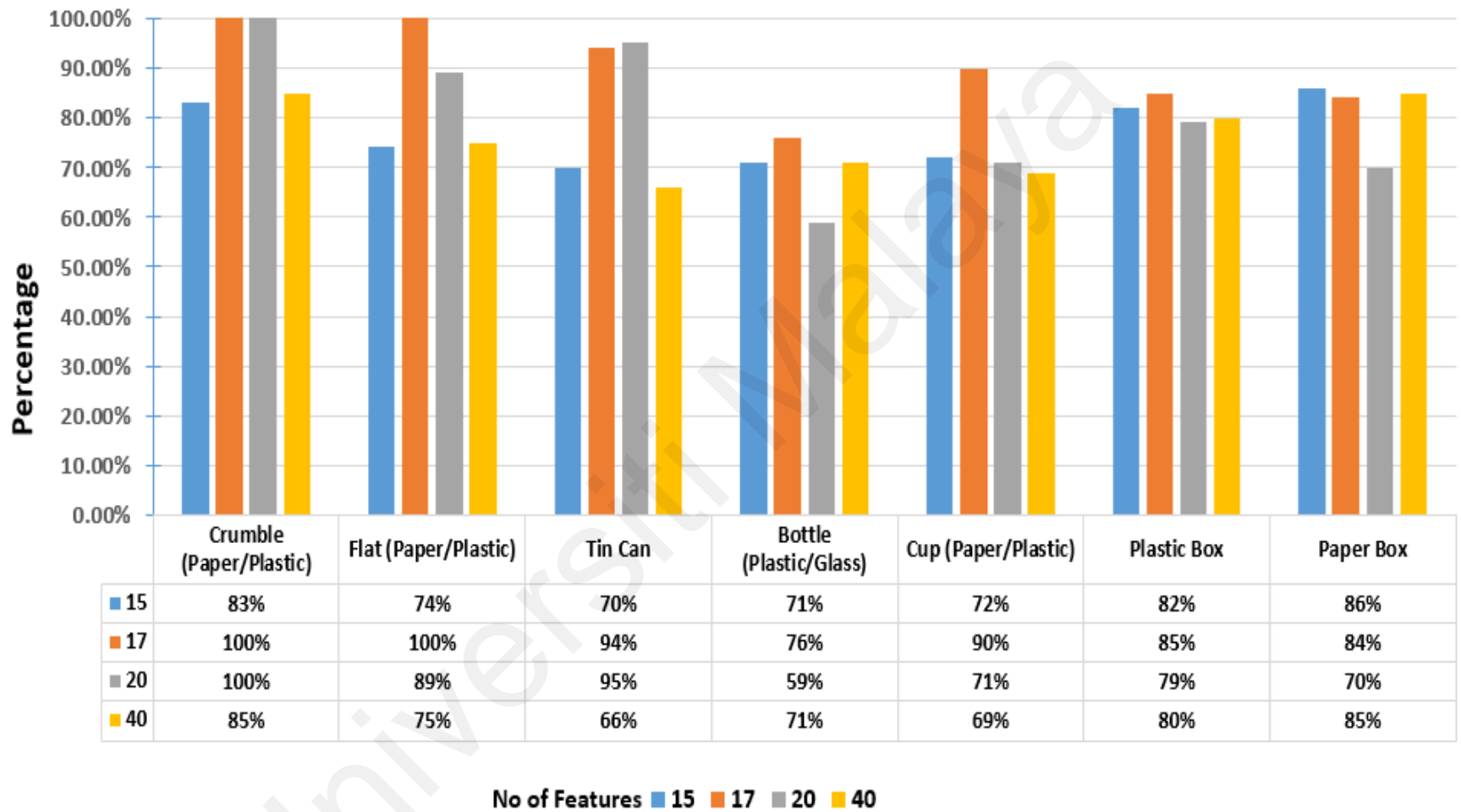


Figure 4.6: Testing Accuracy of each class for 40, 20, 17 and 15 features

CHAPTER 5: CONCLUSION

The goal of this dissertation is to design a suitable classification for mixed waste garbage using image analysis system to sort seven classes of garbage samples. We have demonstrated classification and sorting of garbage from houses, offices and other public places using ASC and GIA system into seven classes i.e., Crumble (Paper/Plastic), Flat (Paper/Plastic), Tin Can, Bottle (Plastic/Glass), Cup (Paper/Plastic), Plastic Box and Paper Box. The system was tested on 320 testing images and the garbage was then sorted in to the respective bins using electro-pneumatic cylinders.

320 images were used for training of the classification model. The classification model Q. Discriminant, Q. SVM, C. SVM, Fine KNN, E. Boosted Trees, E. Bagged Trees were chosen for the training of the dataset. The system originally provided 40 features, but the training accuracy of the classification models were not good. Then we removed unfitting features and made dataset of 20 features. The 20 features best accuracy was 81.42%. Then after several tests three more features were removed from the dataset. 17 features provided highest accuracy for all classification models. The classification model Q. SVM was able to achieve accuracy of 90.69%.

We applied our proposed system to sort the mixed garbage on the conveyor. It has the advantage of using purely vision-based system and automated control system hardware. The Q. SVM classification model was used for testing and the achieved classification accuracy rate was 89.9%.

Our main conclusion is that the effective mix garbage ASC system can be constructed using vision-based system and a simple, straightforward classification algorithm. And the hardware system is not required to be very much delicate. With the microcontroller and electro-pneumatic system, the desired results can be achieved. The most novel aspect of this study is the use of GIA vision system only for selection of image properties which

are the features, based on the images captured by it. We did several tests of the features combinations to achieve the best training accuracy. Results have shown that ASC with GIA system can acquired fitting features for the study and good performance rates can be achieved for the well-suited industry needs.

Future work will concentrate to create more detailed and impactful feature set which can classify the paper and plastic among each other in real time using GIA and ASC systems.

Universiti Malaya

REFERENCES

- Acevedo-Avila, R., Gonzalez-Mendoza, M., & Garcia-Garcia, A. (2016). A Linked List-Based Algorithm for Blob Detection on Embedded Vision-Based Sensors. *Sensors (Basel)*, *16*(6). <https://doi.org/10.3390/s16060782>
- Adedeji, O., & Wang, Z. (2019). Intelligent Waste Classification System Using Deep Learning Convolutional Neural Network. *Procedia Manufacturing*, *35*, 607-612. <https://doi.org/https://doi.org/10.1016/j.promfg.2019.05.086>
- Anzano, J., Casanova, M.-E., Bermúdez, M.-S., & Lasheras, R.-J. (2006). Rapid characterization of plastics using laser-induced plasma spectroscopy (LIPS). *Polymer Testing*, *25*(5), 623-627. <https://doi.org/https://doi.org/10.1016/j.polymeresting.2006.04.005>
- Beyer, C., & Pretz, T. (2004). Special requirements for material characterisation regarding the simulation of solid waste material processing. *Resources, Conservation and Recycling*, *42*(2), 121-131. <https://doi.org/https://doi.org/10.1016/j.resconrec.2004.02.007>
- Burnley, S. J. (2007). The use of chemical composition data in waste management planning – A case study. *Waste Management*, *27*(3), 327-336. <https://doi.org/https://doi.org/10.1016/j.wasman.2005.12.020>
- Cimpan, C., Maul, A., Jansen, M., Pretz, T., & Wenzel, H. (2015). Central sorting and recovery of MSW recyclable materials: A review of technological state-of-the-art, cases, practice and implications for materials recycling. *Journal of Environmental Management*, *156*, 181-199. <https://doi.org/https://doi.org/10.1016/j.jenvman.2015.03.025>
- D, L. I. N., Z, C., M, W., J, Z., & X, Z. (2021, 22-23 Sept. 2021). Design and Implementation of Intelligent Garbage Classification System Based on Artificial Intelligence Technology. 2021 13th International Conference on Computational Intelligence and Communication Networks (CICN),
- Dang, T. L., Cao, T., & Hoshino, Y. (2019). Classification Of Metal Objects Using Deep Neural Networks In Waste Processing Line. *International Journal of Innovative Computing Information and Control*, *15*(5), 1901-1912. <https://doi.org/10.24507/ijicic.15.05.1901>
- Doak, A. G., Roe, M. G., & Kenny, G. R. (2006). Multi-grade object sorting system and method. In: Google Patents.

- Dodbiba, G., & Fujita, T. (2004). Progress in Separating Plastic Materials for Recycling. *Physical Separation in Science and Engineering*, 13, 594923. <https://doi.org/10.1080/14786470412331326350>
- Duan, F., Wang, Y.-N., Liu, H.-J., & Li, Y.-G. (2007). A machine vision inspector for beer bottle. *Engineering Applications of Artificial Intelligence*, 20(7), 1013-1021. <https://doi.org/https://doi.org/10.1016/j.engappai.2006.12.008>
- Edward, & Bruno, M. S. (2000). Automated Sorting of Plastics for Recycling. 3-16.
- Fu, B., Li, S., Wei, J., Li, Q., Wang, Q., & Tu, J. (2021). A Novel Intelligent Garbage Classification System Based on Deep Learning and an Embedded Linux System. *Ieee Access*, 9, 131134-131146. <https://doi.org/10.1109/ACCESS.2021.3114496>
- Gonzalez, R. C., & Woods, R. E. (2008). *Digital Image Processing*. Pearson/Prentice Hall. <https://books.google.co.in/books?id=8uGOnjRGEzoC>
- Gottschling, A., & Schabel, S. (2016). Pattern classification system for the automatic analysis of paper for recycling. *International Journal of Applied Pattern Recognition*, 3(1), 38-58. <https://doi.org/10.1504/ijapr.2016.076986>
- Gundupalli, S. P., Hait, S., & Thakur, A. (2017). Multi-material classification of dry recyclables from municipal solid waste based on thermal imaging. *Waste Management*, 70, 13-21. <https://doi.org/https://doi.org/10.1016/j.wasman.2017.09.019>
- Gundupalli, S. P., Hait, S., & Thakur, A. (2017). A review on automated sorting of source-separated municipal solid waste for recycling [Review]. *Waste Management*, 60, 56-74. <https://doi.org/10.1016/j.wasman.2016.09.015>
- Hannan, M. A., Arebey, M., Begum, R. A., Basri, H., & Al Mamun, M. A. (2016). Content-based image retrieval system for solid waste bin level detection and performance evaluation. *Waste Management*, 50, 10-19. <https://doi.org/https://doi.org/10.1016/j.wasman.2016.01.046>
- Hay, G. J., & Castilla, G. (2008). Geographic Object-Based Image Analysis (GEOBIA): A new name for a new discipline. In T. Blaschke, S. Lang, & G. J. Hay (Eds.), *Object-Based Image Analysis: Spatial Concepts for Knowledge-Driven Remote Sensing Applications* (pp. 75-89). Springer Berlin Heidelberg. https://doi.org/10.1007/978-3-540-77058-9_4
- Hoornweg, D., & Bhada-Tata, P. (2012). *What a Waste : A Global Review of Solid Waste Management* (Vol. 15). World Bank, Washington, DC. © World Bank. .

- Huang, J., Pretz, T., & Bian, Z. (2010, 16-18 Oct. 2010). Intelligent solid waste processing using optical sensor based sorting technology. 2010 3rd International Congress on Image and Signal Processing,
- Huibin Yang, & Yan Juan. (2015). Research on Workpiece Sorting System Based on Machine Vision Mechanism. *Intelligent Control and Automation*, 6(1), 1-9.
- Jiao, Z., & Sun, Y. (2016). A Real-Time Renewable Plastic Particles Sorting Algorithm Based on Image Processing. *MATEC Web of Conferences*, 44, 01049. <https://dx.doi.org/10.1051/mateconf/20164401049>
- Kiran, B. R., Ramakrishnan, K. R., Kumar, Y. S., & Anoop, K. P. (2011, 28-30 Jan. 2011). An improved connected component labeling by recursive label propagation. 2011 National Conference on Communications (NCC),
- Koyanaka, S., & Kobayashi, K. (2010). Automatic sorting of lightweight metal scrap by sensing apparent density and three-dimensional shape. *Resources, Conservation and Recycling*, 54(9), 571-578. <https://doi.org/https://doi.org/10.1016/j.resconrec.2009.10.014>
- Kutilla, M., Viitanen, J., & Vattulainen, A. (2005, 28-30 Nov. 2005). Scrap Metal Sorting with Colour Vision and Inductive Sensor Array. International Conference on Computational Intelligence for Modelling, Control and Automation and International Conference on Intelligent Agents, Web Technologies and Internet Commerce (CIMCA-IAWTIC'06),
- Lachi Reddy, P., Sabiha, S., Jaswitha, k., Dinesh, P., & Naveen, V. (2021). Optimized garbage segregation and monitoring system. *Materials Today: Proceedings*. <https://doi.org/https://doi.org/10.1016/j.matpr.2021.07.256>
- Li, S., Yan, M., & Xu, J. (2020, 28-31 Oct. 2020). Garbage object recognition and classification based on Mask Scoring RCNN. 2020 International Conference on Culture-oriented Science & Technology (ICCST),
- Marques, O. (2011). *Practical Image and Video Processing Using MATLAB*. Wiley. <https://books.google.com.my/books?id=xzD25QEo8qYC>
- Md Mahmudul Hasan Russel, Mehdi Hasan Chowdry, Md.Mehdi Masud Talukder, Md.Shekh Naim Uddin, & Newaz, A. (2013). *Development of Automatic Smart Waste Sensor Machine* International Conference on Mechanical, Industrial and Materials Engineering (ICMIME2013), Rajshahi, Bangladesh.
- O'Toole, M. D., Karimian, N., & Peyton, A. J. (2018). Classification of Nonferrous Metals Using Magnetic Induction Spectroscopy. *IEEE Transactions on Industrial Informatics*, 14(8), 3477-3485. <https://doi.org/10.1109/TII.2017.2786778>

- Özkan, K., Ergin, S., Işık, Ş., & Işıklı, İ. (2015). A new classification scheme of plastic wastes based upon recycling labels. *Waste Management*, 35, 29-35. <https://doi.org/http://dx.doi.org/10.1016/j.wasman.2014.09.030>
- Paluszek, M., & Thomas, S. (2016). *MATLAB Machine Learning*. Apress. <https://books.google.com.my/books?id=3kXODQAAQBAJ>
- Pamintuan, M., Mantiquilla, S. M., Reyes, H., & Samonte, M. J. (2019, 29 Nov.-1 Dec. 2019). i-BIN: An Intelligent Trash Bin for Automatic Waste Segregation and Monitoring System. 2019 IEEE 11th International Conference on Humanoid, Nanotechnology, Information Technology, Communication and Control, Environment, and Management (HNICEM),
- Parfitt, J. P., & Flowerdew, R. (1997). Methodological problems in the generation of household waste statistics: An analysis of the United Kingdom's National Household Waste Analysis Programme. *Applied Geography*, 17(3), 231-244. [https://doi.org/https://doi.org/10.1016/S0143-6228\(96\)00031-8](https://doi.org/https://doi.org/10.1016/S0143-6228(96)00031-8)
- Parker, J. R. (2010). *Algorithms for Image Processing and Computer Vision*. Wiley. <https://books.google.com.my/books?id=BK3oXzpxC44C>
- Rahman, M. O., Hussain, A., Scavino, E., Basri, H., & Hannan, M. A. (2011). Intelligent computer vision system for segregating recyclable waste papers. *Expert Systems with Applications*, 38(8), 10398-10407. <https://doi.org/https://doi.org/10.1016/j.eswa.2011.02.112>
- Rahman, M. O., Hussain, A., Scavino, E., Hannan, M. A., Basri, H., & Ieee. (2012). *Object Identification Using DNA Computing Algorithm*.
- Raj, J. R., Rajula, B. I. P., Tamilbharathi, R., & Srinivasulu, S. (2020, 6-7 March 2020). AN IoT Based Waste Segregator for Recycling Biodegradable and Non-Biodegradable Waste. 2020 6th International Conference on Advanced Computing and Communication Systems (ICACCS),
- Sakr, G. E., Mokbel, M., Darwich, A., Khneisser, M. N., & Hadi, A. (2016, 2-4 Nov. 2016). Comparing deep learning and support vector machines for autonomous waste sorting. 2016 IEEE International Multidisciplinary Conference on Engineering Technology (IMCET),
- Sereda, T. G., & Kostarev, S. N. (2019). Development of automated control system for waste sorting. *IOP Conference Series: Materials Science and Engineering*, 537, 062012. <https://doi.org/10.1088/1757-899x/537/6/062012>

- Shapiro, L. G. (1996). Connected Component Labeling and Adjacency Graph Construction. In T. Y. Kong & A. Rosenfeld (Eds.), *Machine Intelligence and Pattern Recognition* (Vol. 19, pp. 1-30). North-Holland. [https://doi.org/https://doi.org/10.1016/S0923-0459\(96\)80011-5](https://doi.org/https://doi.org/10.1016/S0923-0459(96)80011-5)
- Shapiro, M., & Galperin, V. (2005). Air classification of solid particles: a review. *Chemical Engineering and Processing: Process Intensification*, *44*(2), 279-285. <https://doi.org/https://doi.org/10.1016/j.cep.2004.02.022>
- Shaukat, A., Gao, Y., Kuo, J. A., Bowen, B. A., & Mort, P. E. (2016). Visual classification of waste material for nuclear decommissioning. *Robotics and Autonomous Systems*, *75*, 365-378. <https://doi.org/https://doi.org/10.1016/j.robot.2015.09.005>
- Sofu, M. M., Er, O., Kayacan, M. C., & Cetişli, B. (2016). Design of an automatic apple sorting system using machine vision. *Computers and Electronics in Agriculture*, *127*, 395-405. <https://doi.org/http://dx.doi.org/10.1016/j.compag.2016.06.030>
- Support Vector Machine (SVM)*. Retrieved 04/11 from <https://www.mathworks.com/discovery/support-vector-machine.html>
- Susto, G. A., Schirru, A., Pampuri, S., McLoone, S., & Beghi, A. (2015). Machine Learning for Predictive Maintenance: A Multiple Classifier Approach. *IEEE Transactions on Industrial Informatics*, *11*(3), 812-820. <https://doi.org/10.1109/TII.2014.2349359>
- Tachwali, Y., Al-Assaf, Y., & Al-Ali, A. R. (2007). Automatic multistage classification system for plastic bottles recycling. *Resources, Conservation and Recycling*, *52*(2), 266-285. <https://doi.org/http://dx.doi.org/10.1016/j.resconrec.2007.03.008>
- Tsuchida, A., Kawazumi, H., Kazuyoshi, A., & Yasuo, T. (2009, 25-28 Oct. 2009). Identification of Shredded Plastics in milliseconds using Raman spectroscopy for recycling. 2009 IEEE Sensors,
- Wang, K., & Kong, S. (2011, 20-22 May 2011). Identification method of waste based on gray level co-occurrence matrix and neural network. 2011 International Conference on Materials for Renewable Energy & Environment,
- Xu, L. D., Xu, E. L., & Li, L. (2018). Industry 4.0: state of the art and future trends. *International Journal of Production Research*, *56*(8), 2941-2962. <https://doi.org/10.1080/00207543.2018.1444806>
- Zhang, M.-L., & Zhou, Z.-H. (2007). ML-KNN: A lazy learning approach to multi-label learning. *Pattern Recognition*, *40*(7), 2038-2048. <https://doi.org/https://doi.org/10.1016/j.patcog.2006.12.019>